

Combinatorial connections in snake graphs: Tilings, lattice paths, and perfect matchings

Carolina Melo^a

Submitted: TBD; Accepted: TBD; Published: TBD

© The authors. Released under the CC BY-ND license (International 4.0).

Abstract

Snake graphs and their perfect matchings play a key role in the description of cluster variables of cluster algebras associated to surfaces. In this paper, we introduce triangular snake graphs and establish a bijection between their routes (non-intersecting lattice paths), perfect matchings of their underlying snake graphs, and tilings. As an application, we show that the number of perfect matchings in straight snake graphs can be expressed in terms of determinants of Hankel matrices with Catalan number entries. Moreover, we prove that the number of perfect matchings in snake graphs can be expressed as a sum of products of Fibonacci numbers, and we show how Fibonacci and Pell sequences arise from determinants of matrices with Fibonacci entries.

Mathematics Subject Classifications: 05A19, 05B45, 05C70, 15B36

1 Introduction

In this paper, we introduce triangular snake graphs, a directed acyclic graph structure naturally associated to snake graphs, and use them as a framework to study perfect matchings and their algebraic properties. Our main contributions are:

- We establish a bijection between perfect matchings of a snake graph and k -routes (non-intersecting lattice paths) in its associated triangular snake graph, providing a combinatorial interpretation of classical path-counting results.
- A connection between snake graphs and determinants of Hankel matrices. We establish a connection between the number of perfect matchings in snake graphs and determinants of path matrices involving Catalan, Fibonacci, and Pell numbers, bridging tiling problems with algebraic identities.

^aDepartamento de Matemáticas, Universidad Nacional de Colombia, Bogotá, Colombia
(amelol@unal.edu.co)

1.1 Overview

To place our results in context, we first review classical problems in tiling theory and their connections to combinatorics. Given a region (usually a subset of the Euclidean plane) and a collection of shapes (tiles), a *tiling* of that region is defined as a set of non-overlapping tiles whose union is the region. The study of tilings and their combinatorial properties has been a central topic in discrete mathematics, with deep connections to perfect matchings, continued fractions, and determinant identities; see, for example, [2, 5, 7, 12]. This research often addresses key questions: Is it possible to cover a given region completely using specific tiles? How many distinct ways can such a region be covered without overlapping tiles? Can these tilings be connected to other combinatorial objects through bijections, and what combinatorial properties emerge from these configurations?

As the study of larger regions and more complex tiles progresses, the complexity of these questions increases due to the rapid growth in the number of possible configurations. Nevertheless, progress has been made by focusing on specific families of regions and tiles, yielding precise answers to these questions. A well-known example involves regions defined as subsets of the plane, with tiles being 1×2 rectangles (commonly referred to as dominoes or domino tiles), placed on lattice points. The problem of counting the number of tilings (also called domino tilings) within a given region has been widely studied in mathematics; see, for example, [9, 12]. For instance, the number of domino tilings for a $2 \times n$ rectangle corresponds to the $(n + 1)$ -th Fibonacci number; see [14].

Moreover, combinatorial proofs based on tilings have been used to establish and extend a variety of algebraic identities. Examples include connections with Fibonacci determinants [3], Hankel determinants [8], and the Fibonacci and Pell numbers [13]. The work of Elkies, Kuperberg, Larsen, and Propp in [7] has been foundational in this area. They introduced a family of planar regions called Aztec diamonds and studied their tilings with dominoes. Among their key contributions is the Aztec diamond theorem, which states that the number of domino tilings for this shape is exactly $2^{n(n+1)/2}$. Furthermore, they developed a method to transform tiling problems into the framework of counting paths on graphs. Central to this approach is the concept of a *k-route*, which represents a set of k non-intersecting lattice paths.

Building on the work of Gessel and Viennot [11], Eu and Fu established in [8] connections between determinants of *Hankel matrices* (square matrices in which each ascending skew-diagonal from left to right is constant) and the enumeration of k -tuples of non-intersecting large and small Schröder paths. These bijections establish a link between the domino tilings of Aztec diamonds and non-intersecting lattice paths. An alternative approach to the Aztec diamond theorem, distinct from the methods introduced by Elkies, Kuperberg, Larsen, and Propp, is presented in [6]. In this work, Ciucu obtains the recurrence relation $a_n = 2^n a_{n-1}$ using perfect matchings of cellular graphs. In general, a domino tiling of a region corresponds to a perfect matching in the grid graph obtained by placing a vertex at the center of each square of the region and connecting two vertices whenever their corresponding squares are adjacent.

A *matching* in a graph is defined as a subset of independent edges, *i.e.*, edges that share no common vertices. This concept has been widely studied in mathematics and

computer science due to its broad applications, including graph coloring, flow networks, and neural networks; see, for example, [18]. However, several open problems remain, such as finding a closed formula for the number of matchings in a graph. In particular, determining the number of perfect matchings, denoted as $m(G)$, in an arbitrary graph G remains an unresolved problem. While exact closed formulas are generally unavailable, asymptotic approximations and exact results exist for specific classes of graphs; see, for example, [4, 18].

On the other hand, in the context of cluster algebras associated to surfaces, Musiker, Schiffler, and Williams in [20, 21] established a connection between cluster variables in cluster algebras and perfect matchings of snake graphs (connected planar graphs consisting of a finite sequence of square tiles). Their work provided a formula for computing cluster variables combinatorially. Recently, following the ideas of Eu and Fu, we showed in [19] how to associate a perfect matching of a ladder graph (or straight snake graph, where all tiles lie in a single column or row) to a k -route formed by Schröder paths. In this paper, we extend these ideas by constructing a bijection between perfect matchings and non-intersecting lattice paths, revealing new determinant identities involving some numerical sequences.

We define the region $T(\mathcal{G})$, referred to as the snake graph cover, as the union of all unit squares centered at the vertices of a snake graph \mathcal{G} with d square tiles. Using the domino tilings of $T(\mathcal{G})$, the triangular snake graph $\mathcal{T}_{\mathcal{G}}$ is defined as an acyclic-directed graph with d triangular tiles. Alternatively, employing the edge contraction operation, we provide an alternative method to construct $\mathcal{T}_{\mathcal{G}}$ (see Definition 22). Leveraging Lemma 14 and Definition 17, the set of k -paths p_i from s_i to t_i , where s_1, \dots, s_k is the set of sources and t_1, \dots, t_k is the set of sinks, can be considered. One may then pose the question: How many of these sets of k paths are k -routes? The following synthesis encapsulates Proposition 9, Lemma 19, and Theorem 26 below, providing an answer to this question.

Theorem 1. *Let \mathcal{G} be a snake graph.*

- (1) *There exists a bijection between the domino tilings of the region $T(\mathcal{G})$ and the set $\text{Match}(\mathcal{G})$ of perfect matchings of \mathcal{G} .*
- (2) *The set $\text{Match}(\mathcal{G})$ is in bijection with the set of k -routes from s to t in $\mathcal{T}_{\mathcal{G}}$, where $s = (s_1, \dots, s_k)$ and $t = (t_1, \dots, t_k)$.*

Çanakçı and Schiffler established in [26] that the number of perfect matchings of \mathcal{G} is equal to the numerator of the continued fraction associated with \mathcal{G} . As a consequence, item (1) of the preceding theorem provides a method for determining the number of domino tilings within the region $T(\mathcal{G})$. Moreover, by the Lindström-Gessel-Viennot lemma, which states that the number of k -routes from s to t in $\mathcal{T}_{\mathcal{G}}$ equals the determinant of the corresponding path matrix M_{st} (as seen in Lemma 3), item (2) implies that this determinant can be interpreted as the numerator of the associated continued fraction. Conversely, the continued fraction associated to \mathcal{G} can also be expressed as a quotient of determinants of path matrices.

To establish an explicit connection between snake graphs and Hankel matrices, it is necessary to describe how these combinatorial structures are linked through the study of path matrices and matchings. This exploration reveals a relationship between the entries of such path matrices and well-known numerical sequences, such as the Fibonacci sequence and the Catalan numbers.

The Catalan number sequence, denoted by C , is one of the most important sequences in combinatorics. It has been extensively studied and is associated with over 200 different combinatorial objects; see [24]. This sequence appears in the On-Line Encyclopedia of Integer Sequences (or OEIS) [22] with the identifier A000108 and is recursively defined as follows:

$$C_0 = 1, \quad C_{n+1} = \sum_{i=0}^n C_i C_{n-i}, \quad \text{with } n \geq 0.$$

Examples of combinatorial objects counted by the Catalan numbers include triangulations of convex polygons, binary trees, and Dyck paths; see [23, Corollary 6.2.3].

Similarly, the Fibonacci sequence, denoted by F , is a well-known sequence defined recursively by:

$$F_0 = 0, \quad F_1 = 1, \quad F_{n+1} = F_n + F_{n-1}, \quad \text{for } n > 0.$$

Fibonacci numbers have a wide range of applications in mathematics, computer science, and natural phenomena. They appear in areas such as the golden ratio, population dynamics, and the structure of plants; see, for example, [15].

We explore the combinatorial nature of both Catalan and Fibonacci numbers by connecting them to tiling problems, perfect matchings on snake graphs and Hankel matrices. By extending the concepts of k -routes and perfect matchings, we establish a relationship between these sequences and determinants of matrices associated with snake graphs. In particular, we show how Hankel matrices can be used to study these combinatorial sequences, providing explicit connections between their entries and the number of perfect matchings in specific graph structures. The following synthesis, encompassing Propositions 32, 34, and 37, highlights these relationships:

Theorem 2. *Let C be the sequence of Catalan numbers C_n , and let F_n be the n -th Fibonacci number. Then the following relationship holds:*

$$F_n = \det(H(C)) = \det(M_{st}),$$

where $H(C)$ is a matrix defined in terms of the Hankel matrices of the Catalan numbers, and $M_{st} = (m_{ij})$ is the path matrix associated to the triangular snake graph $\mathcal{T}_{L_{n-2}}$ which corresponds to the vertical ladder graph L_{n-2} .

Additionally, Proposition 34 and Proposition 37 not only address Hankel matrices with entries from the sequence of Catalan numbers but also introduce matrices whose entries are Fibonacci numbers, with determinants matching those of the earlier Hankel matrices. In § 4.2 we explore this property in greater generality, showing that for snake graphs, the number of perfect matchings can be expressed as a sum of products of Fibonacci numbers, described by the determinant of a matrix with entries given in terms of Fibonacci numbers.

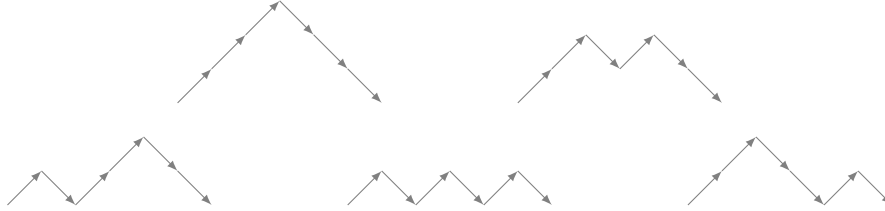
1.2 Organization

The paper is structured as follows. In § 2 we provide the background on lattice paths, Aztec diamonds, Hankel matrices, and snake graphs, and set up the notation that will be used throughout the text. In § 3 we give a bijection between non-intersecting lattice paths (or routes) in an acyclic-directed graph and perfect matchings of the snake graph. We also introduce the triangular snake graph $\mathcal{T}_{\mathcal{G}}$ and describe how each perfect matching corresponds to a k -route of $\mathcal{T}_{\mathcal{G}}$ (§ 3.1). Finally, in § 4 we provide key identities in terms of Fibonacci numbers that allow the computation of determinants of matrices, either Hankel matrices associated with Catalan numbers in the case of straight snake graphs, or more generally, determinants of path matrices.

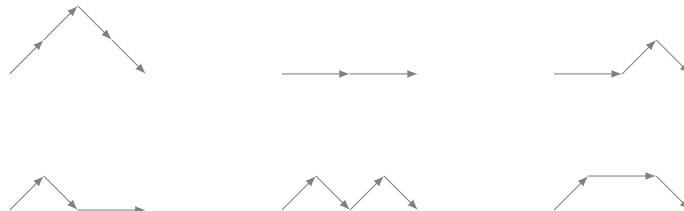
2 Background

2.1 Lattice paths and Aztec diamonds

Let S be a subset of \mathbb{Z}^d . A *lattice path* L in \mathbb{Z}^d of length k with steps in S is a sequence $v_0, v_1, \dots, v_k \in \mathbb{Z}^d$ such that each consecutive difference $v_i - v_{i-1}$ belongs to S . L is said to start at v_0 and end at v_k . The enumeration of these paths often leads to interesting numerical sequences. For example, the set of *Dyck paths* \mathcal{D}_n consists of all lattice paths in \mathbb{Z}^2 from $(0, 0)$ to $(2n, 0)$ for some $n > 0$, using steps $S = \{(1, 1), (1, -1)\}$ without crossing below the x -axis. Their number corresponds to the n -th Catalan number. The following 5 lattice paths make up \mathcal{D}_3 .



Similarly, the (large) Schröder number r_n counts the number of lattice paths from $(0, 0)$ to $(2n, 0)$, for some $n > 0$, using steps $S = \{(1, 1), (1, -1), (2, 0)\}$ and staying above the x -axis. For a fixed n , let S_n denote the set of these *Schröder paths*. The following 6 lattice paths constitute S_2 .



These numbers are intimately connected to tiling problems. The *Aztec diamond* of order n , denoted by $Az(n)$, is defined as the union of all unit squares whose corners have integer coordinates (x, y) that satisfy $|x| + |y| \leq n + 1$. A *domino tile* is a rectangle of size 1 by 2 or 2 by 1 with corners with integer coordinates. A *domino tiling* of $Az(n)$ is a set of non-overlapping dominoes whose union is $Az(n)$. In [7], it was first proven that the number of domino tilings for the Aztec diamond $Az(n)$ is $2^{n(n+1)/2}$. This significant outcome, commonly referred to as the Aztec Diamond Theorem, has been proved in different ways. One such proof was presented by Eu and Fu in [8] using Hankel determinants of the large and small Schröder numbers. This proof relies on a bijection connecting domino tilings of an Aztec diamond to non-intersecting lattice paths. The essential idea behind this bijection involves labeling the rows of $Az(n)$ with numbers from 1 to $2n$ (from bottom to top). For each $1 \leq i \leq n$, a path p_i is defined, starting from the center of the left edge of the i -th row and ending at the center of the right edge of the same row. Whenever the path reaches a high domino, it traverses through the domino, switching from top to bottom or vice versa. For wide dominoes, the path moves horizontally. The dominoes above the highest path are exclusively wide. Therefore, to establish a correspondence between Aztec diamonds and Schröder paths, specific decorated dominoes are introduced. Each domino is depicted as follows:



2.2 Hankel matrices and lattice paths

A well-known problem in linear algebra is the study of *Hankel matrices*, which are $n \times n$ matrices $B = (b_{ij})$ such that, for $i \leq j$, we have $b_{ij} = b_{i+k, j-k}$, for all $k \in [j - i]$. In combinatorics specifically, we study Hankel matrices associated with a sequence $\mathcal{B} = \{b_n\}_{n \in \mathbb{N}}$, which are defined in [1, p.53] as

$$H_n(\mathcal{B}) = \begin{pmatrix} b_0 & b_1 & \cdots & b_{n-1} \\ b_1 & b_2 & \cdots & b_n \\ \vdots & \vdots & \ddots & \vdots \\ b_{n-1} & b_n & \cdots & b_{2n-2} \end{pmatrix} \quad \text{and} \quad H'_n(\mathcal{B}) = \begin{pmatrix} b_1 & b_2 & \cdots & b_n \\ b_2 & b_3 & \cdots & b_{n+1} \\ \vdots & \vdots & \ddots & \vdots \\ b_n & b_{n+1} & \cdots & b_{2n-1} \end{pmatrix}.$$

In particular, the *Hankel determinant* of order n of \mathcal{B} (sometimes called the *Hankel transform*), is the determinant of the corresponding Hankel matrix of order n . The Hankel determinant was first introduced in OEIS with Sloane's sequence A055878 and later studied by Layman [16]. Many interesting properties of Hankel determinants are known. For instance, for the Catalan sequence, we obtain that

$$\det H'_n(C) = \begin{vmatrix} C_1 & C_2 & \cdots & C_n \\ C_2 & C_3 & \cdots & C_{n+1} \\ \vdots & \vdots & \ddots & \vdots \\ C_n & C_{n+1} & \cdots & C_{2n-1} \end{vmatrix} = 1.$$

To find some properties for the determinants of the Hankel matrices associated with the sequence of Catalan numbers we can use the Lindström-Gessel-Viennot lemma. To state this lemma, we first introduce the concepts of routes and path matrices. Let $G = (V, E)$ be a directed graph and let $n \in \mathbb{N}$. A n -vertex $s = (s_1, \dots, s_n)$ of G is an n -tuple where $s_i \in V$, for all $i \in [n]$. If $s = (s_1, \dots, s_n)$ and $t = (t_1, \dots, t_n)$ are n -vertices of G , define a n -path (also called *path system*) $P = (p_1, \dots, p_n)$ from s to t , where p_i is a path from s_i to t_i .

If the paths p_i and p_j do not have vertices in common, for $1 \leq i, j \leq n$, they are *vertex-disjoint paths*. The n -path $R = (p_1, \dots, p_n)$ is a n -route if p_i and p_j are vertex-disjoint, for all $i \neq j$. Let A be a commutative ring and let $w : E \rightarrow A$ be a weight function on the edges of a directed graph G .

The *weight* of a n -route R , denoted as $w(R)$, is the product of the weights of the edges in the paths:

$$w(R) = \prod_{i=1}^n \prod_{e \in p_i} w(e).$$

The *path matrix* $M_{st} = (m_{ij})_{1 \leq i, j \leq n}$ between two n -vertices $s = (s_1, \dots, s_n)$ and $t = (t_1, \dots, t_n)$ is defined as follows:

$$m_{ij} = \sum_{p: s_i \rightarrow t_j} w(p).$$

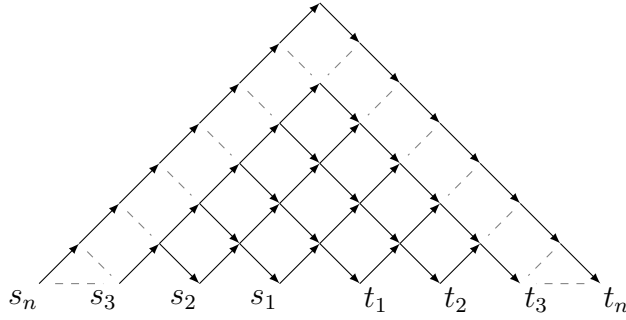
In particular, if $w(e) = 1$ for all edges $e \in E$ (unweighted graph), the path matrix $M_{st} = (m_{ij})_{1 \leq i, j \leq n}$ from $s = (s_1, \dots, s_n)$ to $t = (t_1, \dots, t_n)$ is such that m_{ij} is equal to the number of paths from s_i to t_j .

Lemma 3 (Lindström [17], Gessel-Viennot [11, Theorem 1]). *Let G be an acyclic directed unweighted graph, and let $s = (s_1, \dots, s_n)$ and $t = (t_1, \dots, t_n)$ be two n -vectors of G , then*

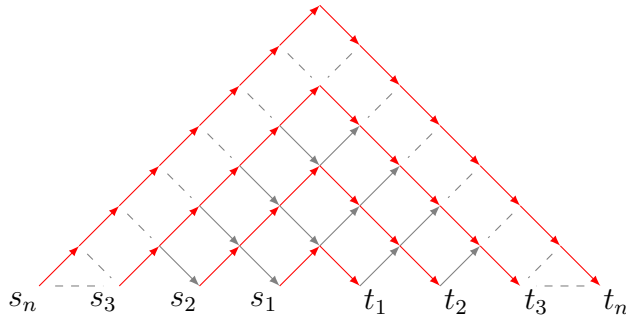
$$\det M_{st} = |\{R : R \text{ is a } n\text{-route from } s \text{ to } t\}|,$$

where M_{st} is the path matrix between s and t .

An example relating the previous concepts is given by the graph below with n -vertices $s = (s_1, \dots, s_n)$ and $t = (t_1, \dots, t_n)$



According to the picture, the paths from s_i to t_k are Dyck paths, in this way, the path matrix is $M_{st} = (m_{ij})$, where $m_{ij} = C_{i+j-1}$, which is the Hankel matrix $H'_n(C)$ associated to the sequence C of Catalan numbers. Additionally, only the n -route is the following



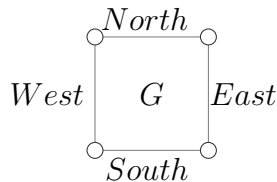
Therefore, using the Lemma 3, we conclude that $\det H'_n(C) = 1$.

2.3 Perfect matchings and snake graphs

In [25] and [26] the authors introduced a useful relationship between the continued fraction associated with a snake graph, the number of perfect matchings of such graph and a cluster algebra. These relationships became a tool to simplify some problems related to each of these objects, and they are one of the main interests of the present work.

Let $G = (V, E)$ be a graph with $|V| = n$ and let $S \subset E$. The set S is said to be a *matching* on G , if these edges do not have vertices in common. If each vertex in G is incident to an edge of S , then S is a *perfect matching* and $|S| = \frac{n}{2}$. We denote by $\text{Match}(G)$ the set of perfect matchings of G .

We consider a tile G as a graph that has the following form:



A *snake graph* \mathcal{G} is a connected planar graph consisting of a finite sequence of tiles G_1, G_2, \dots, G_d , with $d \geq 1$, in such a way that for each $i \in [d - 1]$, the G_i and G_{i+1} tiles

share exactly one edge e_i , which is the North edge of G_i and the South edge of G_{i+1} , or the East edge of G_i and the West edge of G_{i+1} . The edges e_i that are contained in two tiles are called *interior edges*. For a snake graph made up of tiles G_1, G_2, \dots, G_d , the interior edges are e_1, e_2, \dots, e_{d-1} . All of the other edges are called *boundary edges*.

Each snake graph \mathcal{G} admits a sign function $f : E(\mathcal{G}) \rightarrow \{+, -\}$ such that for each tile G_i in \mathcal{G} the following conditions are met:

- The north and west edges of G_i have the same sign,
- The south and east edges of G_i have the same sign,
- The sign of the north edge is opposite to the sign of the south edge.

These signs determine a continued fraction associated to \mathcal{G} , encoding combinatorial properties of its perfect matchings. If \mathcal{G} is a snake graph with d tiles, then we define the sequence of signs

$$[f(e_0), f(e_1), \dots, f(e_{d-1}), f(e_d)],$$

where e_1, \dots, e_{d-1} are the interior edges of \mathcal{G} , e_0 is the south edge of G_1 and e_d is the north edge of G_d . If $\epsilon \in \{+, -\}$ we have

$$[f(e_0), f(e_1), \dots, f(e_{d-1}), f(e_d)] = \underbrace{[\epsilon, \dots, \epsilon]}_{a_1}, \underbrace{[-\epsilon, \dots, -\epsilon]}_{a_2}, \dots, \underbrace{[\pm\epsilon, \dots, \pm\epsilon]}_{a_n}, \quad (1)$$

then the continued fraction $[a_1, \dots, a_n]$ associated to \mathcal{G} is obtained, where

$$[a_1, \dots, a_n] = a_1 + \frac{1}{a_2 + \frac{1}{a_3 + \frac{1}{\dots + \frac{1}{a_n}}}}.$$

Now let $[a_1, \dots, a_n]$ be a positive continued fraction (*i.e.*, if each $a_i \in \mathbb{Z}_{>0}$). The snake graph associated to the continued fraction $[a_1, \dots, a_n]$ is denoted by $\mathcal{G}[a_1, \dots, a_n]$ and is the snake graph with $d = a_1 + a_2 + \dots + a_n - 1$ tiles determined by the sign sequence 1. The following theorem relates the continued fractions of a snake graph with its perfect matchings.

Theorem 4 ([26]). *If $m(\mathcal{G})$ denotes the number of perfect matchings of \mathcal{G} then*

$$[a_1, a_2, \dots, a_n] = \frac{m(\mathcal{G}[a_1, a_2, \dots, a_n])}{m(\mathcal{G}[a_2, \dots, a_n])}.$$

As an application of Theorem 4, we note that the numerator of the continued fraction of $[a_1, \dots, a_n]$ corresponds to the number of perfect matchings in the snake graph $\mathcal{G}[a_1, \dots, a_n]$. Similarly, the numerator of $[a_n, \dots, a_1]$ represents the number of perfect matchings in $\mathcal{G}[a_n, \dots, a_1]$. Since these two snake graphs are identical up to a 180-degree rotation, they must have the same number of perfect matchings. This leads to the following result.

Theorem 5 ([26]). *The continued fractions $[a_1, \dots, a_n]$ and $[a_n, \dots, a_1]$ have the same numerator.*

Observe that if $[a_1, \dots, a_n]$ is a continued fraction with $a_n = 1$, then $[a_1, \dots, a_n] = [a_1, \dots, a_{n-1} + 1]$. This property, along with Theorem 5, will be used in § 4.2.

3 Perfect matchings, tilings and non-intersecting lattice paths

In this section, we will construct an acyclic-directed graph corresponding to each snake graph. This construction will establish a bijection between the routes (non-intersecting lattice paths) in the resulting acyclic-directed graph and the perfect matchings of the snake graph. This construction was motivated by the bijection between domino tilings of an Aztec diamond and non-intersecting lattice paths (large Schröder paths satisfying some particular conditions) given by Eu and Fu in [8].

3.1 Tilings and snake graphs

Without loss of generality and for an easier exposition, let us consider a snake graph \mathcal{G} formed by a sequence of unit squares G_1, G_2, \dots, G_d , where $d \geq 1$.

Definition 6. The *cover* $T(G_i)$ of tile G_i in a snake graph \mathcal{G} is the union of all unit squares centered at the vertices of G_i . The *snake graph cover* $T(\mathcal{G})$ of a snake graph \mathcal{G} is the union of the covers of all tiles G_i in \mathcal{G} .

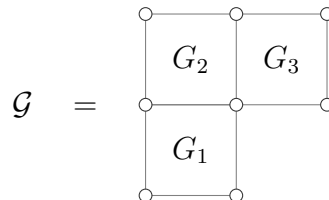


Figure 1: From left to right, tile G_i of a snake graph \mathcal{G} and its cover $T(G_i)$.

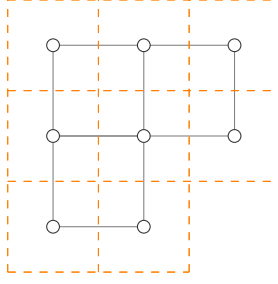
The unit square centered at the southwest vertex of the tile G_1 is called the *initial tile* of $T(\mathcal{G})$.

Definition 7. A *domino tile* is formed by the union of any two unit squares sharing an edge. A *snake graph tiling* of \mathcal{G} is a set of non-overlapping domino tiles whose union forms $T(\mathcal{G})$. We denote the set of all snake graph tilings of \mathcal{G} by $\text{Til}(\mathcal{G})$.

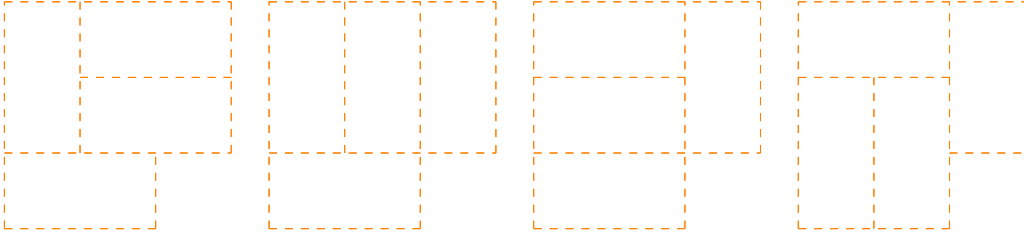
Example 8. Consider the snake graph



The snake graph cover $T(\mathcal{G})$ corresponding to it is



There exist precisely four snake graph tilings of \mathcal{G}



Proposition 9. *Let \mathcal{G} be a snake graph. There exists a bijection between the set $Til(\mathcal{G})$ of snake graph tilings of \mathcal{G} and the set $Match(\mathcal{G})$ of perfect matchings of \mathcal{G} .*

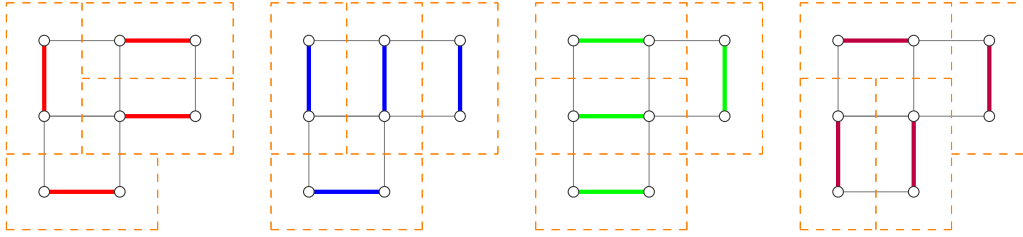
Proof. Given $P \in Match(\mathcal{G})$, we associate a snake graph tiling as follows: For an edge e_{ij} in P connecting the vertices v_i and v_j in \mathcal{G} , we create a domino tile D_{ij} associated to e_{ij} by linking the unit squares centered at v_i and v_j . If two distinct edges e_{ij} and e_{kl} exist in P , the intersection of the domino tiles D_{ij} and D_{kl} is empty. Otherwise, the existence of a common vertex between e_{ij} and e_{kl} would contradict the assumption of P being a matching of \mathcal{G} . Moreover,

$$\bigcup_{e_{ij}} D_{ij} = T(\mathcal{G}),$$

where the union is taken over all edges e_{ij} in P . This holds because for each edge e_{kl} in P , there exists a tile G_i in \mathcal{G} such that e_{kl} is an edge of G_i , and thus $D_{kl} \subset T(G_i) \subset T(\mathcal{G})$. Furthermore, as P is a perfect matching, for each cover $T(G_i)$ there exist edges e_{pq} in P such that $T(G_i) \subseteq \bigcup_{e_{pq}} D_{pq}$. Conversely, considering a snake graph tiling of \mathcal{G} , for every vertex v_p of \mathcal{G} , there exists a unique domino tile such that v_p is the center of one of the unit squares contained in that domino tile. Let v_q be the center of the other unit square. We construct a perfect matching P where the edge e_{pq} from v_p to v_q is an edge of P .

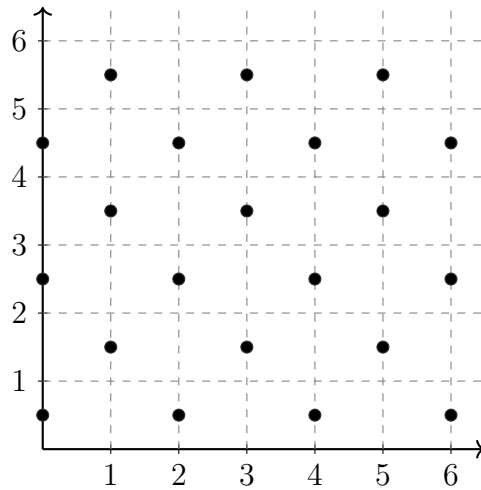
This proves the bijection between snake graph tilings and perfect matchings in \mathcal{G} . \square

Example 10. Let \mathcal{G} the snake graph in the Example 8. Then, the perfect matchings associated to the four snake graph tilings are



3.2 Decorated snake graph tilings and paths

We intend to establish a correspondence between routes and snake graph tilings. To achieve this, we define a grid in $(\mathbb{R}_{\geq 0})^2$, placing black points at coordinates $(2n, 2m + 0.5)$ and $(2n + 1, 2m + 1.5)$, where n and m are elements of \mathbb{N} .



Subsequently, we position the snake graph cover $T(\mathcal{G})$ of \mathcal{G} on the grid, ensuring that the southwest vertex of the initial tile of $T(\mathcal{G})$ aligns with $(0, 0)$, thus establishing a decoration using black points within the snake graph cover. We can observe that the snake graph cover is decorated with the following two unit squares

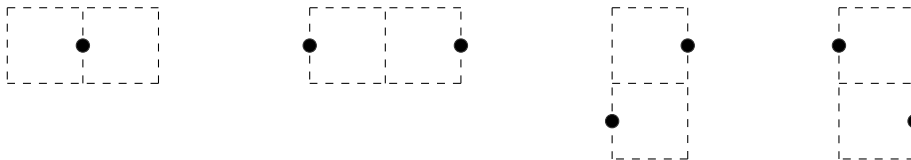
Right-decorated square



Left-decorated square



in such a way that the initial tile of $T(\mathcal{G})$ is left-decorated, and each square that shares an edge with a left-decorated square is right-decorated, and vice versa. In this way, any domino tile in a snake graph tiling will be decorated in one of the following ways



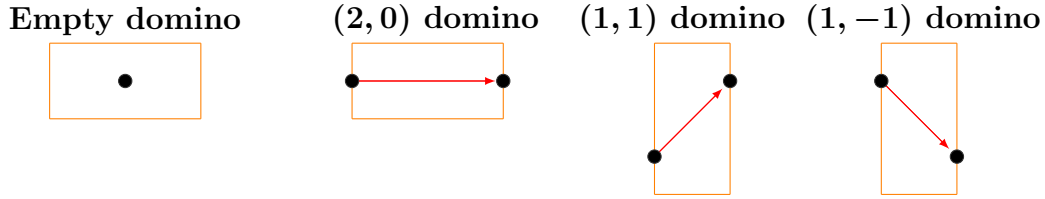


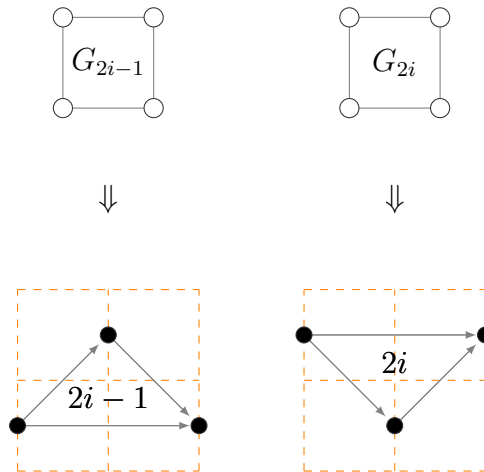
Figure 2: Decorated dominoes.

So decorated dominoes can be naturally associated to these figures as follows:

Remark 11. While the coordinates of the black points in the grid are not aligned with integers on the y -axis, a simple translation by 0.5 units downwards shows that the resulting grid does indeed possess integer coordinates. Based on this observation, we classify each of the paths derived from the decorated snake graph tilings as a lattice path with steps $S = \{(2, 0), (1, 1), (1, -1)\}$.

Definition 12. The *triangular snake graph* $\mathcal{T}_{\mathcal{G}}$ associated to \mathcal{G} is a connected acyclic-directed graph derived from the decorated snake graph cover. It is constructed by placing an arrow between two distinct black points if the corresponding unit squares share an edge as shown in Figure 2.

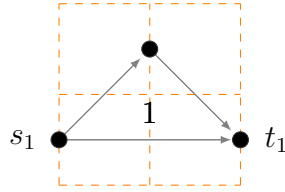
Remark 13. Notably, the black points that belong to only one square in $T(\mathcal{G})$ are sources or sinks. Considering that the arrows in the triangular snake graph are oriented from left to right, the sources (resp. the sinks) reside on a domino tile's left-hand side (resp. right-hand side). Additionally, note that every tile G_j of \mathcal{G} contributes a triangular tile labeled by the number j , depending on the parity of j , as follows:



We will now prove some other not-so-obvious properties about $\mathcal{T}_{\mathcal{G}}$.

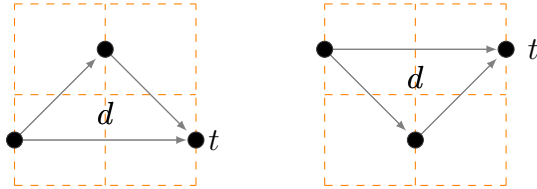
Lemma 14. Let $\mathcal{T}_{\mathcal{G}}$ be the triangular snake graph associated to \mathcal{G} . Then $\mathcal{T}_{\mathcal{G}}$ possesses an equal number of sources and sinks.

Proof. The proof proceeds by induction on the number of tiles in \mathcal{G} . For the base case when $d = 1$, $\mathcal{G} = G_1$, then the triangular snake graph $\mathcal{T}_{\mathcal{G}}$ associated to G_1 is depicted as:



In this case, there exists one source s_1 and one sink t_1 . Assume the statement holds for any snake graph with d tiles, $d > 1$. We will now establish its validity for a snake graph \mathcal{G}_{d+1} containing $d + 1$ tiles.

Consider the snake graph \mathcal{G}_d obtained by removing the last tile G_{d+1} from \mathcal{G}_{d+1} . By the induction hypothesis, $\mathcal{T}_{\mathcal{G}_d}$ has an equal number of sources and sinks. Now, we examine two possible scenarios for the last part of the triangular snake graph of \mathcal{G}_d :



If tiles G_d and G_{d+1} share the edge e_d , where e_d is the north edge of G_d and the south edge of G_{d+1} , we obtain two possible different structures:

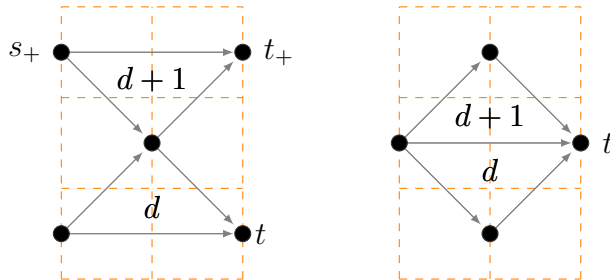


Figure 3: Triangular tiles associated to the tiles G_d and G_{d+1} that share the north and south edge.

In the first case, the resulting triangular snake graph of \mathcal{G}_{d+1} encompasses all the sources and sinks of \mathcal{G}_d . Additionally, two new elements are introduced: a source s_+ and a sink t_+ as depicted in the left of Figure 3. Conversely, in the second case, the sources and sinks in both \mathcal{G}_d and \mathcal{G}_{d+1} are equal. This distinction arises due to the structural differences between the configurations of adjoining tiles.

On the other hand, if the tiles G_d and G_{d+1} share the edge e_d , where e_d is the east edge of G_d and the west edge of G_{d+1} , we obtain one of the following scenarios

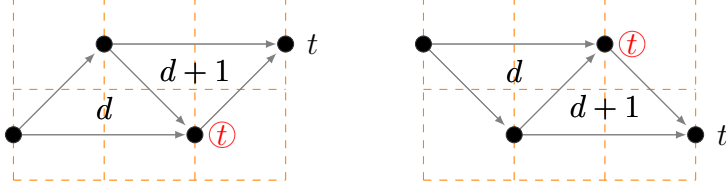


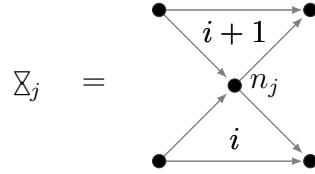
Figure 4: Triangular tiles associated to the tiles G_d and G_{d+1} that share the east and west edge.

Upon close examination, it becomes evident that the element identified as the sink t in \mathcal{G}_d is no longer a sink of $\mathcal{T}_{\mathcal{G}_{d+1}}$. Instead, the southeast black point within the new triangular tile takes over the role previously attributed to the mentioned sink.

In either case, the count of sources and sinks remains equal, thereby completing the proof. \square

The proof of Lemma 14 yields an additional insight: the number of sources and sinks increases with the appearance of a specific subgraph within the triangular snake graph. This subgraph is formally defined in the following definition.

Definition 15. An *hourglass graph* is a graph with the following structure:



The vertex n_j will be called the *neck* of the hourglass graph \mathbb{X}_j . The triangular subgraphs labeled by $i+1$ and i are the *head* and *body* of \mathbb{X}_j , respectively.

As a direct consequence, we establish the following corollary.

Corollary 16. Let $\mathcal{T}_{\mathcal{G}}$ be the triangular snake graph associated to \mathcal{G} . $\mathcal{T}_{\mathcal{G}}$ contains $k-1$ hourglass graphs as subgraphs if and only if the number of sources (and sinks) in $\mathcal{T}_{\mathcal{G}}$ is k , where $k \geq 1$.

Proof. The proof follows a similar structure as the proof of Lemma 14 and will only be indicated briefly. We proceed by induction based on the number of sources in $\mathcal{T}_{\mathcal{G}}$. For the base case, when $\mathcal{T}_{\mathcal{G}}$ has no hourglass graphs, the number of sources (and sinks) is 1. When $\mathcal{T}_{\mathcal{G}}$ has only one hourglass graph, the number of sources (and sinks) is 2. Assuming the validity of the statement for any triangular snake graph with $k-1$ hourglasses, we aim to establish its validity for a triangular snake graph $\mathcal{T}_{\mathcal{G}}$ containing k hourglasses.

Let us consider the triangular snake graph $\mathcal{T}_{\mathcal{G}}^-$ obtained by removing the triangular tiles labeled by i from $\mathcal{T}_{\mathcal{G}}$, for $i > j$, where j is the label of the body of the last hourglass \mathbb{X}_k . Then, $\mathcal{T}_{\mathcal{G}}^-$ contains $k-1$ hourglass graphs. According to the induction hypothesis,

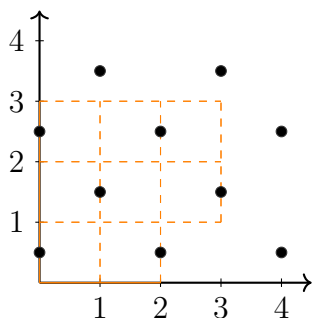
$\mathcal{T}_{\mathcal{G}}^-$ possesses k sources (and sinks). A similar analysis to that in the proof of Lemma 14, shows that $\mathcal{T}_{\mathcal{G}}$ has $k + 1$ sources (and sinks). To prove the reverse implication, assume $\mathcal{T}_{\mathcal{G}}$ contains k sources (and sinks). By induction on the number of sources, the same reasoning can be applied to show that $\mathcal{T}_{\mathcal{G}}$ contains $k - 1$ hourglass graphs as subgraphs. \square

Unless stated otherwise, we assume that $\mathcal{T}_{\mathcal{G}}$ possesses k sources, denoted as s_1, \dots, s_k , and k sinks, denoted as t_1, \dots, t_k . To describe the k -routes of $\mathcal{T}_{\mathcal{G}}$, these k -vertices of $\mathcal{T}_{\mathcal{G}}$ are defined as follows.

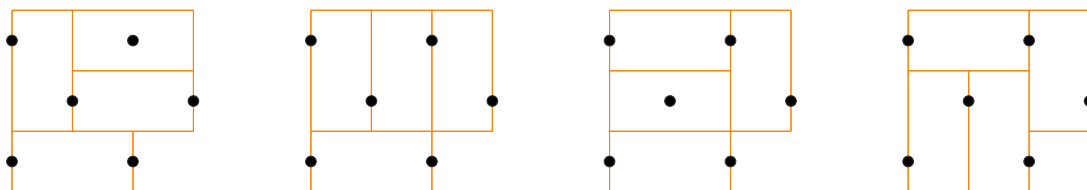
Definition 17. The k -vertices $s = (s_1, \dots, s_k)$ and $t = (t_1, \dots, t_k)$ of $\mathcal{T}_{\mathcal{G}}$ are defined by imposing the following conditions:

1. $\mathcal{T}_{\mathcal{G}}$ contains $k - 1$ hourglass graphs as subgraphs.
2. $s = (s_1, \dots, s_k)$ and $t = (t_1, \dots, t_k)$ are ordered vectors formed by the sources and sinks in $\mathcal{T}_{\mathcal{G}}$, respectively.
3. If s_i and s_j (respectively t_i and t_j) are vertices such that $i < j$, then the y-coordinate of s_i (respectively t_i) is less than the y-coordinate of s_j (respectively t_j).

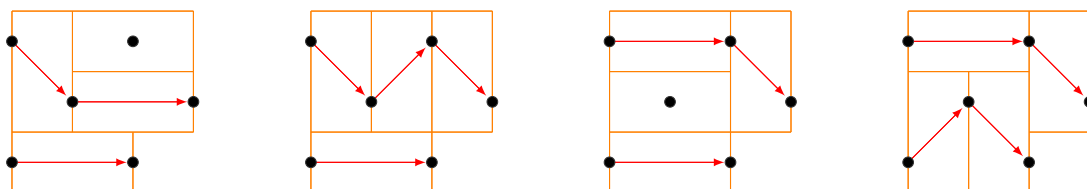
Example 18. Let \mathcal{G} the snake graph in the Example 8. The snake graph cover on the grid is depicted as follows:



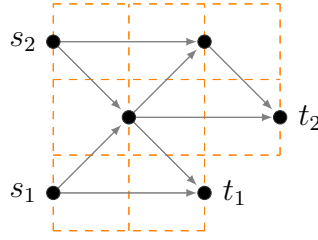
The snake graph tilings are



Then, we obtain the following decorated snake graph tilings associated to perfect matchings depicted in Example 10



and the triangular snake graph \mathcal{T}_G with its 2-vertices, $s = (s_1, s_2)$ and $t = (t_1, t_2)$, is



We can observe that each decorated snake graph tiling contains two paths that do not intersect. Additionally, the paths start at vertex s_i and end at vertex t_i , for some $i \in \{1, 2\}$.

Lemma 19. *Let $P \in \text{Match}(\mathcal{G})$. Then the decorated snake graph cover associated to P represents a k -route from s to t in \mathcal{T}_G .*

Proof. Let $p = (v_{l+1}|\alpha_l, \alpha_{l-1}, \dots, \alpha_1|v_1)$ be a maximal path in the decorated snake graph tiling associated to $P \in \text{Match}(\mathcal{G})$ such that p starts at vertex v_1 and ends at vertex v_{l+1} . There exist l decorated domino tiles with steps $(2, 0)$, $(1, 1)$ or $(1, -1)$ in such a way that every arrow α_i of p corresponds to one of these decorated domino tiles. We claim that v_1 is a source and v_{l+1} is a sink in \mathcal{T}_G . Otherwise, if v_1 is not a source, then it would be on the right-hand side of a domino tile D_{v_1} , leading to two possible cases:

1. D_{v_1} is an empty domino. This case contradicts the requirement that consecutive horizontal black points should maintain a distance of 2 units, not one.
2. D_{v_1} is a $(2, 0)$, $(1, 1)$, or $(1, -1)$ domino. This case breaches the requirement that p is a maximal path starting at v_1 in the decorated snake graph tiling associated to P .

Similarly, if v_{l+1} is not a sink, it would be on the left-hand side of a domino tile $D_{v_{l+1}}$, and the same two cases apply as for v_1 . Consequently, there must exist $i, j \in [k]$ such that $v_1 = s_i$ and $v_{l+1} = t_j$.

It is now necessary to prove that indeed $i = j$. Suppose $i \neq j$. Then, p traverses an hourglass graph in one of the three ways shown on the left of Figure 5.

If any of these cases were to occur, the perfect matching P would have the edge configurations illustrated in one of the three cases on the right side of Figure 5. However, by parity considerations, this situation is not possible, as both the right and left sides of P would inevitably contain at least one unmatched vertex. Consequently, none of these cases results in a valid perfect matching, affirming that any path p in the decorated snake graph tiling associated to a perfect matching P starts at a source s_i and ends at a sink t_i .

Moreover, consider two paths p and p' where p starts at s_i and ends at t_i , while p' starts at s_j and ends at t_j . If $s_i \neq s_j$ and $t_i \neq t_j$, their intersection at a vertex v implies the existence of α and α' on p and p' , respectively, such that v is a common vertex of

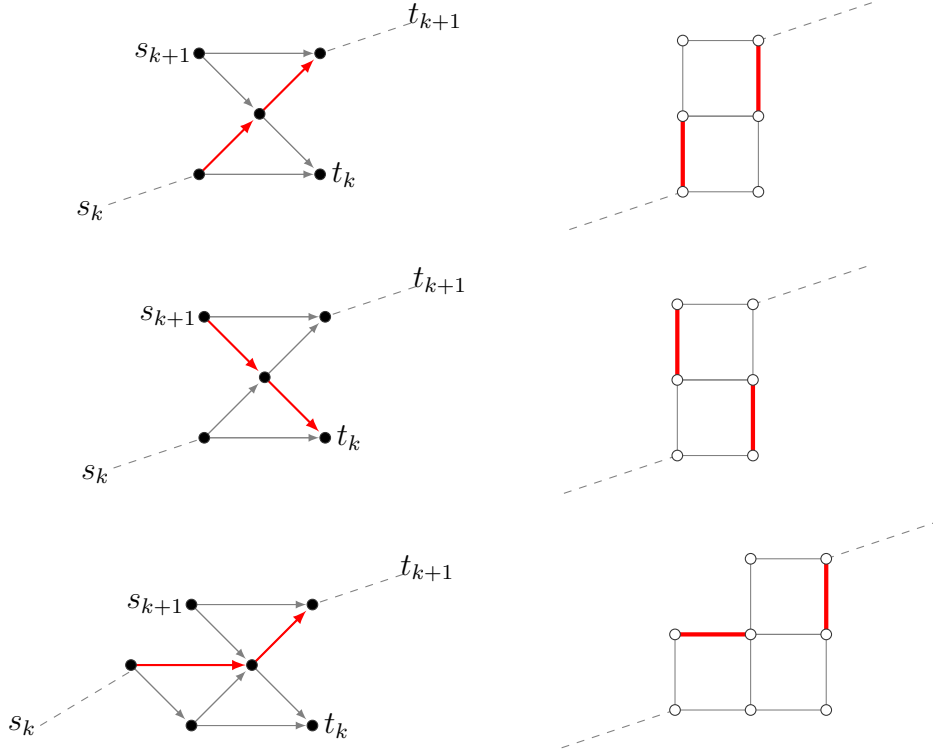


Figure 5: The 3 cases in which p is a path starting at s_i and ending at t_j , $i \neq j$.

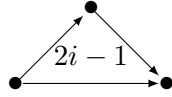
both arrows. This contradicts the requirement that the domino tiles containing α and α' must be non-overlapping, as imposed by the snake graph tiling.

Hence, we have proved that the paths in the snake graph tiling are paths exclusively from s_i to t_i , for $i \in [k]$, and these paths are vertex-disjoint. Therefore, each perfect matching provides a unique k -route from s to t in \mathcal{T}_G , thereby completing the proof. \square

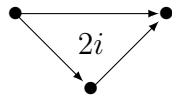
Remark 20. It is evident that if we consider two distinct perfect matchings, their respective k -routes will differ. Specifically, if e is an edge present in the perfect matching P but absent in the perfect matching P' , then the k -route R_P will contain a decorated domino (either an empty, $(2, 0)$, $(1, 1)$ or a $(1, -1)$ domino) that is not present in $R_{P'}$. In the cases where the domino in R_P that is absent in $R_{P'}$ is a $(2, 0)$, $(1, -1)$, or $(1, 1)$ domino, then the corresponding arrow will be absent in $R_{P'}$. In the case where the empty edge formed by squares centered on the vertices v_1 and v_2 (where they are right-decorated and left-decorated squares, respectively) is present in R_P , we observe that in $R_{P'}$ there exist two dominoes ($(2, 0)$, $(1, 1)$ or a $(1, -1)$) D_1 and D_2 , in such a way that the square centered at v_1 is in D_1 , and the square centered at v_2 is in D_2 . Consequently, the arrows corresponding to D_1 and D_2 are present in $R_{P'}$ but absent in R_P .

3.3 Edge contraction in snake graphs

Now, we are going to consider Remark 13. Again we consider a snake graph \mathcal{G} , which is built by the sequence of tiles G_1, G_2, \dots, G_d , with $d \geq 1$. If d is an even number (resp. an odd number), then tiles G_{2i-1} , with $i \in \{1, 2, \dots, \lfloor d/2 \rfloor\}$ (resp. $i \in \{1, 2, \dots, \lfloor d/2 \rfloor + 1\}$) will be identified with the subgraph

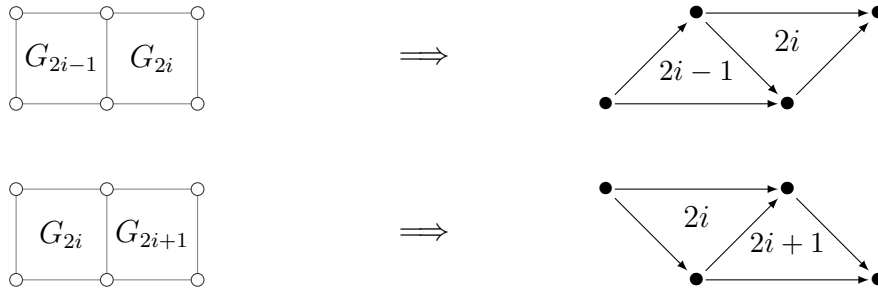


and the tiles G_{2i} , with $i \in \{1, 2, \dots, \lfloor d/2 \rfloor\}$ will be identified with the subgraph

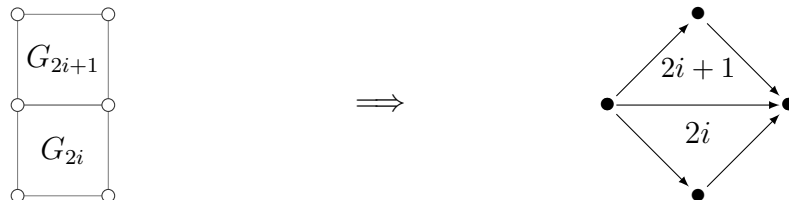


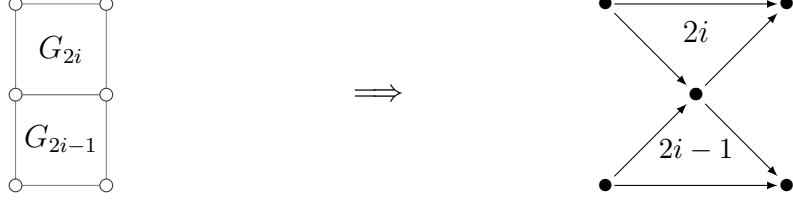
Then the acyclic-directed graph $\mathcal{T}_{\mathcal{G}}$ is formed by the following rules:

1. If the tiles G_j and G_{j+1} of the snake graph \mathcal{G} are joined by their east and west sides, then the respective triangles labeled by j and $j+1$ are joined by the arrows corresponding to the steps $(1, 1)$ and $(1, -1)$ as follows:



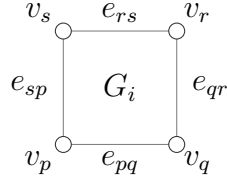
2. If the tiles G_j and G_{j+1} of the snake graph \mathcal{G} are joined by their north and south sides, then the respective triangles labeled by j and $j+1$ are joined by their north and south arrows (corresponding to steps $(1, 0)$) or by their north and south vertices, as follows:





We can see that the construction of $\mathcal{T}_{\mathcal{G}}$ is very similar to that of \mathcal{G} , except for the shape of the tiles (the square tiles are changed to triangular tiles). Therefore, making use of the operation in graph theory called edge contraction, and thinking about maintaining the information alluding to the cluster variables seen in § 2.3, we are going to make a different construction than the one introduced in § 3.1.

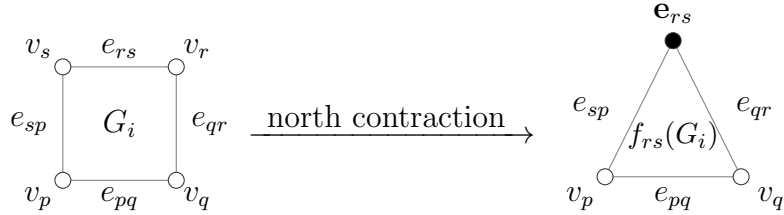
Definition 21. Let \mathcal{G} a snake graph and let $G_i = (V_i, E_i)$ a tile of \mathcal{G} , where $V_i = \{v_p, v_q, v_r, v_s\}$ and $E_i = \{e_{pq}, e_{qr}, e_{rs}, e_{sp}\}$:



Let f_{rs} be a function that maps every vertex in $V_i - \{v_r, v_s\}$ to itself, and otherwise maps v_r and v_s to a new vertex \mathbf{e}_{rs} . We define the *north contraction* of G_i as a new graph $f_{rs}(G_i) = (\hat{V}_i, \hat{E}_i)$, where

$$\hat{V}_i = (V_i - \{v_r, v_s\}) \cup \{\mathbf{e}_{rs}\} \quad \text{and} \quad \hat{E}_i = E_i - \{e_{rs}\},$$

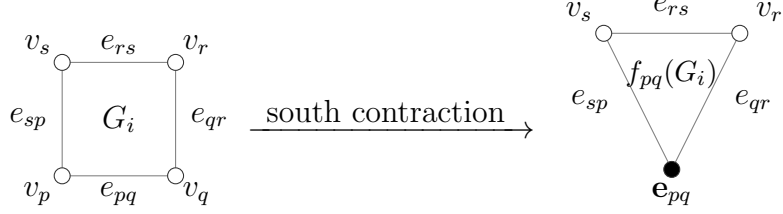
and for every $v \in V_i$, we have that $f_{rs}(v) \in \hat{V}_i$ is incident to an edge $e \in \hat{E}_i \subset E_i$ if and only if e is incident to v in G_i .



Analogously, let f_{pq} be a function that maps every vertex in $V_i - \{v_p, v_q\}$ to itself, and otherwise, maps v_p and v_q to a new vertex \mathbf{e}_{pq} . We define the *south contraction* of G_i as a new graph $f_{pq}(G_i) = (\check{V}_i, \check{E}_i)$, where

$$\check{V}_i = (V_i - \{v_p, v_q\}) \cup \{\mathbf{e}_{pq}\} \quad \text{and} \quad \check{E}_i = E_i - \{e_{pq}\},$$

and for every $v \in V_i$, we have that $f_{pq}(v) \in \check{V}_i$ is incident to an edge $e \in \check{E}_i \subset E_i$ if and only if e is incident to v in G_i .



If no confusion arises, any north contraction (resp. south contraction) will be called f_N (resp. f_S).

Definition 22. Let \mathcal{G} be a snake graph with d tiles and interior edges e_1, e_2, \dots, e_{d-1} . The *contracted snake graph* associated to \mathcal{G} is a connected planar graph consisting of a finite sequence of tiles T_1, T_2, \dots, T_d in such a way that

1. $T_i = f_N(G_i)$ if i is odd, and otherwise, $T_i = f_S(G_i)$ if i is even.
2. For each $i \in [d-1]$, T_i and T_{i+1} share exactly the edge e_i or the vertex \mathbf{e}_i .

The *oriented contracted snake graph* is obtained when we put orientations to the edges of the contracted snake graph with the condition that the arrows are oriented from left to right.

Remark 23. In order to generate equivalent lattice paths in the oriented contracted snake graph, as discussed in § 3.1 for $\mathcal{T}_{\mathcal{G}}$ and characterized by steps from the set

$$\{(2, 0), (1, 1), (1, -1)\},$$

we can consider an isomorphic snake graph to \mathcal{G} in Definition 22 with tiles G_i as 1×2 rectangles. Consequently, the oriented contracted snake graph of \mathcal{G} is canonically isomorphic to the triangular snake graph $\mathcal{T}_{\mathcal{G}}$. Therefore, we systematically identify these graphs. Hence we can think of $\mathcal{T}_{\mathcal{G}}$ either as a triangular snake graph or as an oriented contracted snake graph. The k -vertices $s = (s_1, \dots, s_k)$ and $t = (t_1, \dots, t_k)$ (as defined in Definition 17) are also considered within this context.

Lemma 24. *Let $\mathcal{T}_{\mathcal{G}}$ be the oriented contracted snake graph of \mathcal{G} . The sinks and sources are the only vertices that are not the result of contractions of edges of \mathcal{G} .*

Proof. This directly follows from Definition 21. If \mathbf{e}_{pq} represents the contraction of the edge e_{pq} within a tile G_i of \mathcal{G} , then the west and east edges of G_i are incidents to \mathbf{e}_{pq} , with the west arrow directed into \mathbf{e}_{pq} and the east arrow directed out of \mathbf{e}_{pq} . Consequently, the vertices obtained through edge contractions cannot serve as sources or sinks. Moreover, any other vertex is obtained by an edge contraction as it is either the top or the bottom of a triangular tile. \square

Remark 25. A *decontraction* process can be applied to $\mathcal{T}_{\mathcal{G}}$ to reconstruct the snake graph \mathcal{G} from $\mathcal{T}_{\mathcal{G}}$. According to Lemma 24, the sources, sinks, and their incident arrows remain unchanged. However, for each vertex \mathbf{e} in $\mathcal{T}_{\mathcal{G}}$ that is neither a source nor a sink, two

new vertices, v_e and v'_e , along with the edge e , are introduced. The arrows that end at \mathbf{e} become incident to the vertex v_e , while those that start at \mathbf{e} will be incident to the vertex v'_e . Formally, this process is defined as follows: Let $\mathcal{T}_{\mathcal{G}} = (\overline{V}, \overline{E})$ be the oriented contracted snake graph associated to \mathcal{G} . Denote by S the set of sources and sinks in $\mathcal{T}_{\mathcal{G}}$. Let h be a function that maps every vertex \mathbf{e} in $V - S$ to a new arrow $v_e \xrightarrow{e} v'_e$. Define the sets:

$$V' = \bigcup_{\mathbf{e} \in \overline{V} - S} \{v_e, v'_e\} \quad \text{and} \quad E' = \bigcup_{\mathbf{e} \in \overline{V} - S} \{h(\mathbf{e})\} = \bigcup_{\mathbf{e} \in \overline{V} - S} \{e\}.$$

Then, $\overrightarrow{\mathcal{G}} = (V, E)$ is such that $V = (\overline{V} - S) \cup V'$ and $E = \overline{E} \cup E'$. For every arrow $\alpha \in \overline{E}$ such that $s(\alpha) = \mathbf{e}$, the corresponding arrow $\alpha \in E$ satisfies $s(\alpha) = v_e$; otherwise, if $\alpha \in \overline{E}$ is such that $t(\alpha) = \mathbf{e}$, then $\alpha \in E$ satisfies $t(\alpha) = v'_e$. The underlying graph of $\overrightarrow{\mathcal{G}}$ (i.e., without considering the direction of the arrows) is the snake graph \mathcal{G} .

Theorem 26. *Let \mathcal{G} be a snake graph. The set of perfect matchings $\text{Match}(\mathcal{G})$ of \mathcal{G} is in bijection with the set of k -routes from s to t in $\mathcal{T}_{\mathcal{G}}$.*

Proof. According to Lemma 19, every perfect matching $P \in \text{Match}(\mathcal{G})$ gives rise to a k -route from s to t in $\mathcal{T}_{\mathcal{G}}$. It is sufficient to prove that for every k -route R , we can obtain a perfect matching P_R and that different k -routes give rise to different perfect matchings. We think of $\mathcal{T}_{\mathcal{G}}$ as the oriented contracted snake graph associated to \mathcal{G} and consider the decontraction process and the notation described in Remark 25. Consider a k -route R from s to t in $\mathcal{T}_{\mathcal{G}}$. We consider the following subsets of arrows and vertices in $\mathcal{T}_{\mathcal{G}}$:

1. Let $T \subseteq \overline{E}$ be the set of all arrows α in $\mathcal{T}_{\mathcal{G}}$ such that α belongs to a path p of R .
2. Let $U \subseteq \overline{V} - S$ be the set of all non-source or non-sink vertices \mathbf{e} in $\mathcal{T}_{\mathcal{G}}$ such that \mathbf{e} does not belong to a path of R .

We claim that the edges associated to T and U obtained after the decontraction process form a perfect matching P_R of \mathcal{G} . First, we will show that all vertices in \mathcal{G} belong to an edge of the decontraction process of $T \cup U$. This is evident because the vertices of $\mathcal{T}_{\mathcal{G}}$ are sources, sinks, or contractions of edges. In the first two cases, for every source s_i and sink t_i there exists a path in the k -route R starting at s_i and ending at t_i . Therefore, all sources and sinks belong to the edges obtained by the decontraction process of T . In the third case, every vertex \mathbf{e} obtained by contraction of an edge belongs to the edges obtained by the decontraction process of T , provided \mathbf{e} belongs to a path of R ; or \mathbf{e} belongs to the edges obtained by the decontraction process of U , in case \mathbf{e} does not belong to a path of R .

Now, we aim to show that for any two distinct edges e and e' in the decontraction process of $T \cup U$, e and e' do not share common vertices. For every path

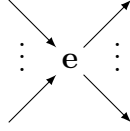
$$p_i = s_i \xrightarrow{\alpha_1} \mathbf{e}_1 \xrightarrow{\alpha_2} \mathbf{e}_2 \xrightarrow{\alpha_3} \dots \xrightarrow{\alpha_{l-1}} \mathbf{e}_{l-1} \xrightarrow{\alpha_l} t_i$$

in R , we obtain the following edges when we apply the decontraction process.

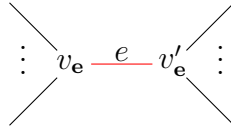
$$s_i \xrightarrow{\alpha_1} v_{\mathbf{e}_1} \xrightarrow{e_1} v'_{\mathbf{e}_1} \xrightarrow{\alpha_2} v_{\mathbf{e}_2} \xrightarrow{e_2} v'_{\mathbf{e}_2} \xrightarrow{\alpha_3} \dots \xrightarrow{\alpha_{l-1}} v_{\mathbf{e}_{l-1}} \xrightarrow{e_{l-1}} v'_{\mathbf{e}_{l-1}} \xrightarrow{\alpha_l} t_i$$

where the red edges $\alpha_1, \alpha_2, \dots, \alpha_l$ are edges in P_R , while the gray arrows e_1, e_2, \dots, e_{l-1} are not. There is no other edge in P_R that shares a vertex with the edges $\alpha_1, \dots, \alpha_l$. Otherwise, there would exist a path p_j in R that shares a vertex with p_i , it would contradict the fact that R is a k -route.

On the other hand, for every edge contraction vertex \mathbf{e} that does not belong to a path of R



we obtain the following edges when we apply the decontraction process



where the red edge e is an edge in P_R , and all incident edges to e do not belong to P_R . Therefore, P_R is a perfect matching of \mathcal{G} .

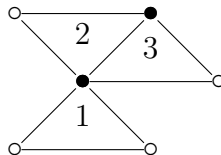
Finally, let us consider two distinct k -routes, denoted as R and R' . We observe that their corresponding perfect matchings, namely P_R and $P_{R'}$, are distinct. This follows directly from the existence of an arrow α in a path of R that is absent in any path of R' . According to the definitions of P_R and $P_{R'}$, the edge corresponding to α is included in P_R but not in $P_{R'}$. Consequently, P_R and $P_{R'}$ differ. \square

Corollary 27. *The number of perfect matchings $m(\mathcal{G})$ of the snake graph \mathcal{G} is equal to the determinant of the path matrix of $\mathcal{T}_{\mathcal{G}}$ between the k -vertices $s = (s_1, \dots, s_k)$ and $t = (t_1, \dots, t_k)$.*

Proof. The result follows immediately from Theorem 26 and Lemma 3. \square

This result establishes a strong connection between combinatorial structures in snake graphs and determinant formulas. In the next section, we explore how these path matrices are related to Hankel matrices, a fundamental class of matrices that encode classical number sequences such as Fibonacci and Catalan numbers. By leveraging these connections, we derive new determinant identities that reveal deeper algebraic properties of snake graphs.

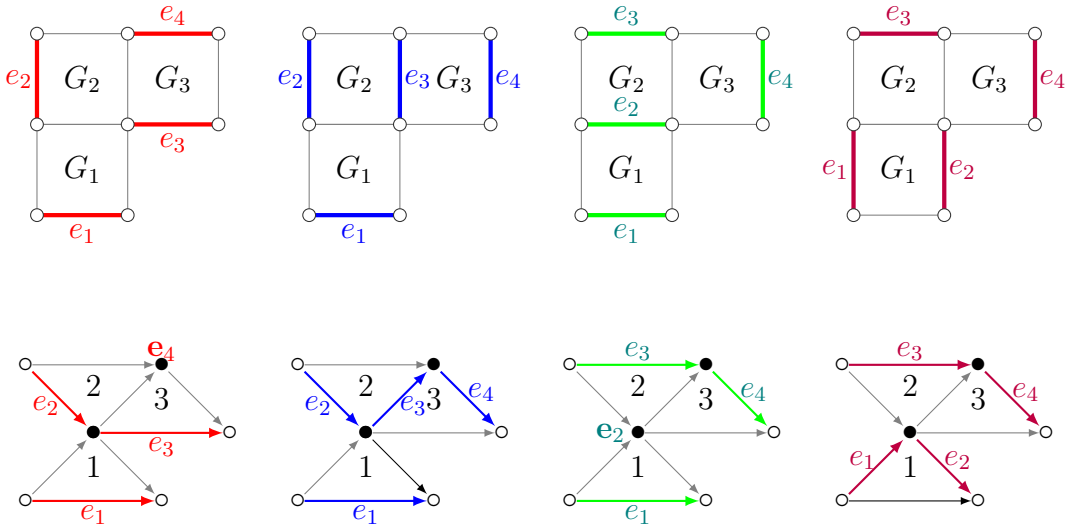
Example 28. Consider the snake graph of Example 8. Its contracted snake graph is depicted as follows.



and its oriented contracted snake graph and associated path matrix are illustrated as follows:

$$\mathcal{T}_{\mathcal{G}} = \begin{array}{c} s_2 \circ \xrightarrow{2} \bullet \\ \searrow \quad \nearrow \\ \bullet \xrightarrow{3} t_2 \circ \\ \nearrow \quad \searrow \\ s_1 \circ \xrightarrow{1} t_1 \circ \end{array} \quad M_{st} = \begin{pmatrix} 2 & 2 \\ 1 & 3 \end{pmatrix}.$$

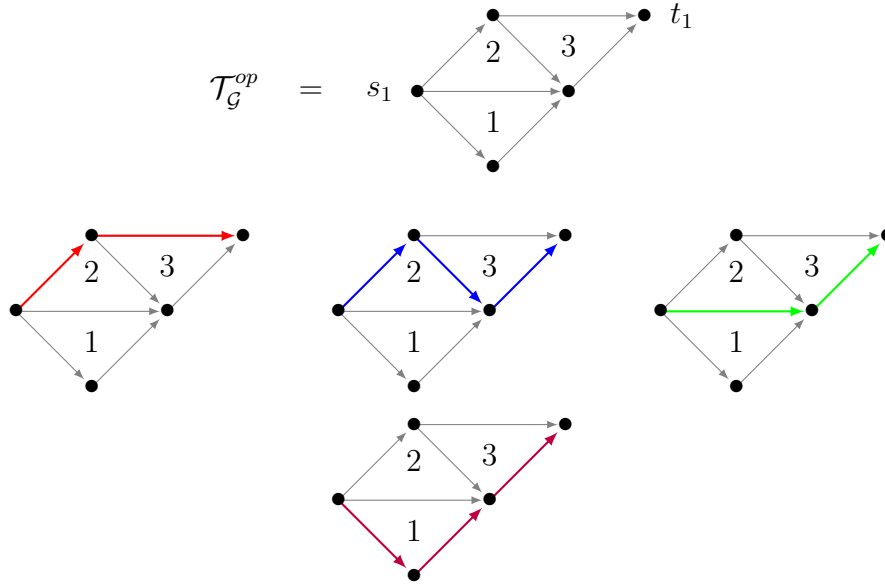
The number of perfect matchings equals the determinant of M_{st} . There exist 4 perfect matchings in \mathcal{G} , each corresponding to distinct 2-routes in $\mathcal{T}_{\mathcal{G}}$, which are:



We observe that when examining the contracted snake graph corresponding to a perfect matching, it aligns with the k -route immediately below it. Likewise, applying the decontraction process to a k -route yields the perfect matching that lies above it.

Remark 29. Note that in Definition 22, the assignment of northern and southern contractions to odd and even indices is arbitrary. One could equally well consider the opposite assignment, where northern contractions are associated with even indices and southern contractions with odd indices. Although the resulting contracted snake graphs are different with potentially varying numbers of sources and sinks, the number of routes remains invariant. Moreover, the bijection between the perfect matchings and the routes of the contracted snake graph obtained by this opposite assignment can still be established. Throughout this paper, we will consider both constructions, as the combinatorial properties of one may be more convenient than the other, depending on the desired formulas for counting paths or routes.

Example 30. Consider the snake graph of Example 8. Its contracted snake graph $\mathcal{T}_{\mathcal{G}}$ is depicted in Example 28. If we consider the opposite assignment, where northern contractions are associated with even indices and southern contractions with odd indices, we obtain the following triangular snake graph $\mathcal{T}_{\mathcal{G}}^{op}$ and corresponding routes



4 Fibonacci identities and Hankel matrices

4.1 Identities in straight snake graphs

In this section, our primary objective is to identify matrices exhibiting an "equivalence" to particular families of Hankel matrices based on lattice paths. This exploration intends to present instances where simpler acyclic graphs can be identified. These graphs provide a more straightforward approach for determining the entries of the path matrix and computing specific determinants. In particular, in this subsection, we work with a special class of snake graphs known as ladder graphs before addressing the general case. We fix the following notation:

Definition 31. A ladder graph L_n is defined as a straight snake graph with n tiles.

Following the construction from the previous section, in the next proposition, we consider a directed acyclic graph that contains as a subgraph the triangular snake graph associated with a ladder graph. Later, we will see that this subgraph preserves the same number of paths as the graph considered in the proposition derived from Aztec diamonds.

Proposition 32. Let C be the sequence of Catalan numbers C_n and let F_n be the n -th Fibonacci number. Then the following relationship holds:

$$\det(H_k(C) + H'_k(C)) = F_{2k+1},$$

where $H_k(C)$ and $H'_k(C)$ are the Hankel matrices of the Catalan numbers.

Proof. The main idea of this proof is to identify a suitable graph that enables us to employ Lemma 3, thereby equating the requested determinant with the number of paths in the said graph. Notably, each component of the matrix counts the number of lattice paths

in \mathbb{Z}^2 that start at $(0,0)$ and end at $(2n,0)$, and the number of lattice paths that start at $(0,0)$ and end at $(2n+2,0)$. Observe that in the acyclic-directed graph in Figure 6, there are precisely $C_{i+j-2} + C_{i+j-1}$ paths from the vertex s_i to the vertex t_j . Therefore,

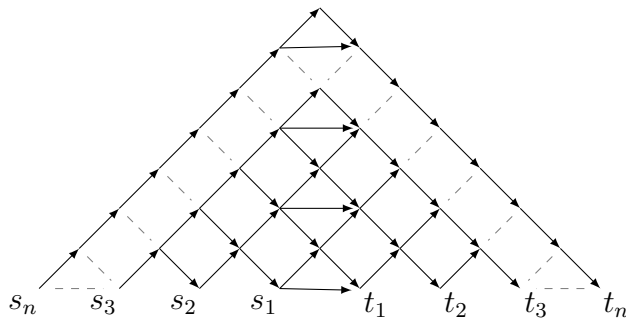
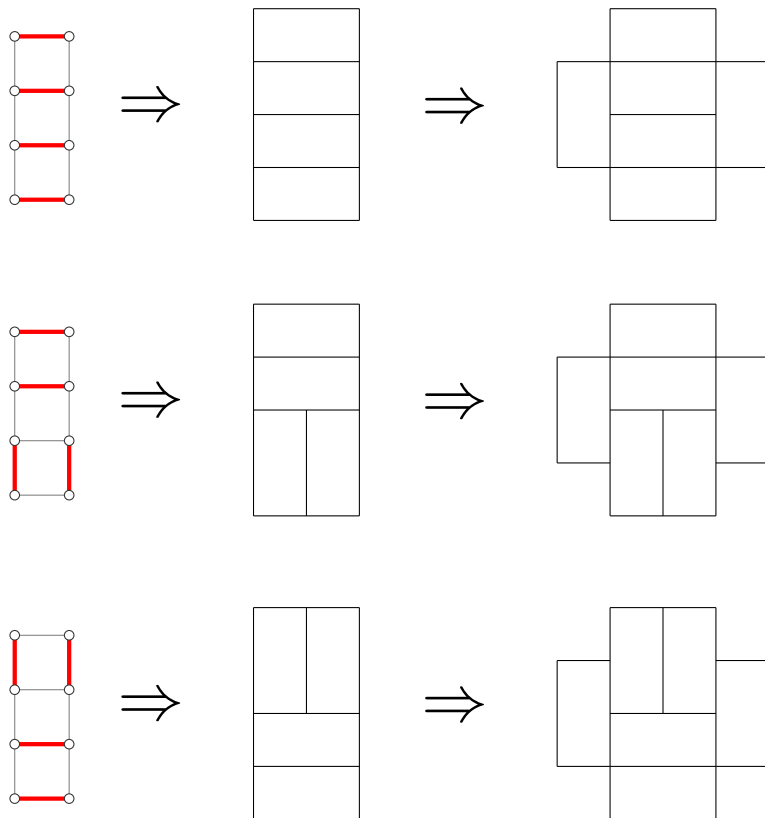
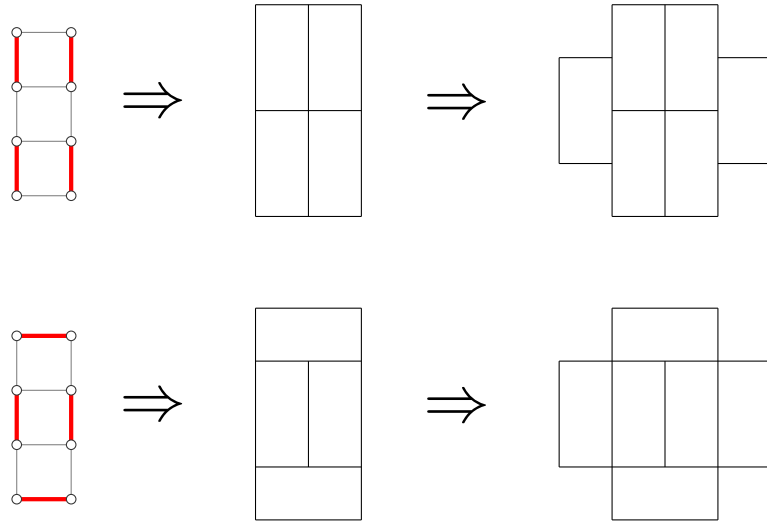


Figure 6: Catalan acyclic-directed graph associated to n -routes.

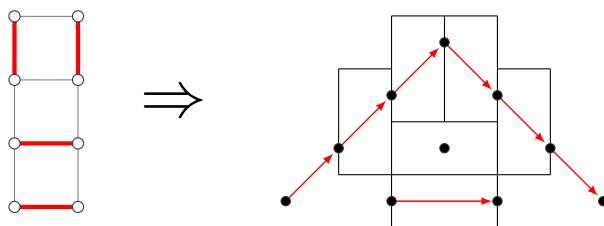
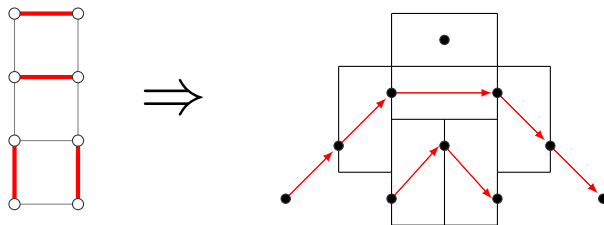
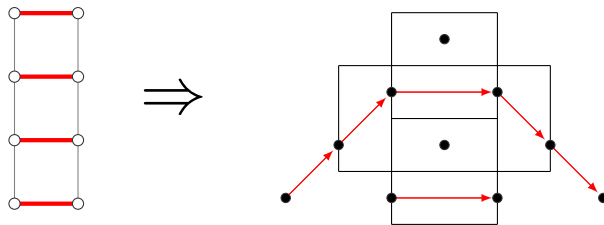
the requested determinant counts the n -routes from s to t in the aforementioned graph. These paths correspond to the Aztec diamonds defined in 2.1, which, in turn, are linked to perfect matchings. Consequently, the result follows immediately. \square

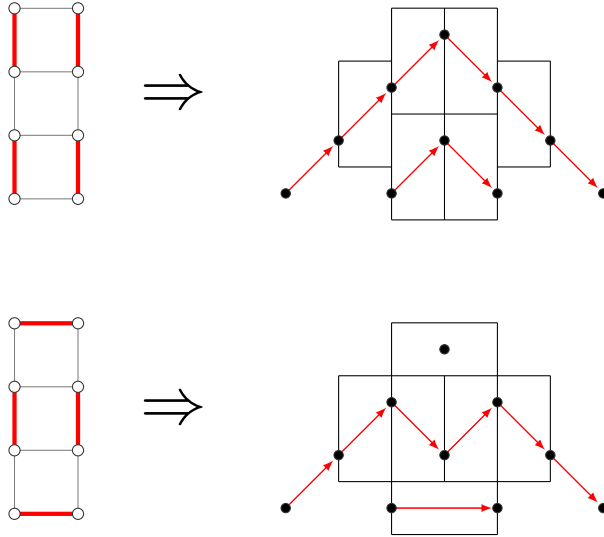
Example 33. For the five perfect matchings of L_3 we obtain the following domino tiling of $Az(2)$:





Therefore, we have the following routes for each perfect matching.





Therefore, the acyclic-directed graph in Figure 7 is constructed by superimposing every one of the previously obtained routes. The acyclic-directed graph in Figure 7 allows us to

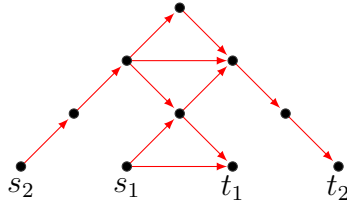


Figure 7: Acyclic-directed graph constructed by superimposing 2-routes.

add arrows as long as they do not affect the number of 2-routes. For instance, we can add two arrows as shown in Figure 8 (one ending at vertex s_1 and another starting at vertex t_1). This is because 2-routes are a collection of two vertex-disjoint paths. Since the path from s_1 to t_1 shares vertices with the new arrows, the path from s_2 to t_2 cannot intersect it.

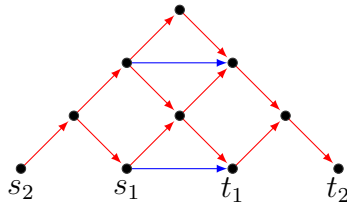


Figure 8: Catalan acyclic-directed graph associated to 2-routes.

To find the entries of the path matrix, the color of the horizontal arrows was changed to blue in Figure 8. If we want to see the paths from vertex s_i to vertex t_j , then we can

see that the number of paths that use a blue edge is C_{i+j-2} , and the number of paths that do not use those blue edges is C_{i+j-1} . Therefore, the path matrix is

$$M_2 = \begin{pmatrix} C_0 + C_1 & C_1 + C_2 \\ C_1 + C_2 & C_2 + C_3 \end{pmatrix} = \begin{pmatrix} 2 & 3 \\ 3 & 7 \end{pmatrix}$$

where it can easily be verified that $\det(M_2) = 5$.

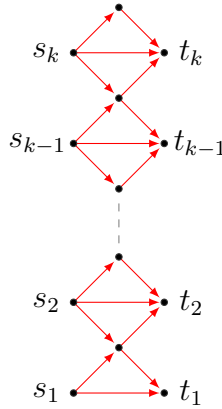
Proposition 34. *Let $M_{st} = (m_{ij})_{1 \leq i, j \leq k}$ be the path matrix associated to the triangular snake graph of the vertical ladder graph L_{2k-1} , $k \geq 1$, and let F_n be the n -th Fibonacci number. Then the following relationship holds*

$$\det M_{st} = F_{2k+1},$$

where

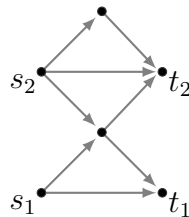
$$m_{ij} = \begin{cases} F_3 = 2 & \text{if } i = j = 1; \\ F_4 = 3 & \text{if } i = j \in \{2, \dots, k\}; \\ F_2 = 1 & \text{if } i = j + 1 \text{ or } i = j - 1; \\ F_0 = 0 & \text{otherwise.} \end{cases}$$

Proof. Consider the vertical ladder graph L_{2k-1} . We obtain the following triangular snake graph $\mathcal{T}_{L_{2k-1}}$

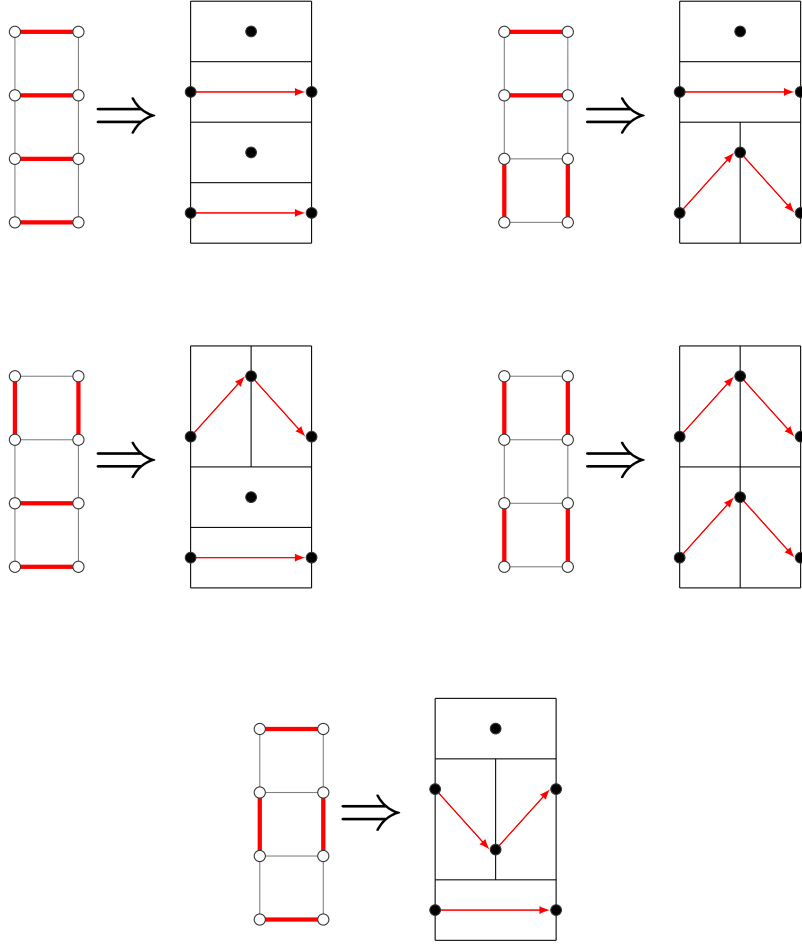


From a direct inspection we can see that the number m_{ii} of paths p_i from s_i to t_i is equal to 3 if $i \in \{2, 3, \dots, k\}$ and equal to 2 if $i = 1$. In addition, the number m_{ij} of paths from s_i to t_j is equal to 1 if $|i - j| = 1$ and equal to 0 if $|i - j| > 1$. Then, using Lemma 3 we conclude the proposition. \square

Example 35. Consider the ladder graph L_3 of the Example 33. The triangular snake graph can be represented as follows:



We obtain the following perfect matchings and their corresponding 2-routes



Then comparing Proposition 32 with Proposition 34 we obtain

$$\begin{vmatrix} C_0 + C_1 & C_1 + C_2 \\ C_1 + C_2 & C_2 + C_3 \end{vmatrix} = \begin{vmatrix} 2 & 3 \\ 3 & 7 \end{vmatrix} = F_5 = \begin{vmatrix} 2 & 1 \\ 1 & 3 \end{vmatrix} = \begin{vmatrix} F_3 & F_2 \\ F_2 & F_4 \end{vmatrix}.$$

Remark 36. Based on the earlier finding, we can discern that the Hankel matrix discussed in Proposition 32 shares an identical determinant with the matrix presented in Proposition 34. Although both matrices exhibit similarities in terms of determinants, it is noteworthy to highlight the contrast in their components. The former matrix encompasses a total of k^2 non-zero entries, while the latter matrix boasts a more compact structure with only $3k - 2$ non-zero entries.

This discrepancy in the number of non-zero entries underscores a notable difference in the structures of these matrices. Exploring such differences might provide valuable insights into the underlying structures and relationships in Hankel matrices and contribute to the broader understanding of their significance in mathematical theory and applications.

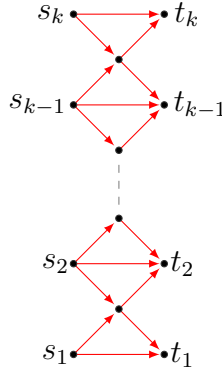
Proposition 37. Let $M_{st} = (m_{ij})_{1 \leq i, j \leq k}$ be the path matrix associated to the triangular snake graph of the vertical ladder graph L_{2k-2} , where $k \geq 1$. Let C be the sequence of Catalan numbers C_n and let F_n be the n -th Fibonacci number. Then the following relationship holds:

$$\det M_{st} = F_{2k} = \det (H_k(C) + H'_k(C) - E_{k,k}),$$

where $E_{i,j}$ is the matrix whose (i, j) -th entry is 1 and all other entries are zero, $H_k(C)$ and $H'_k(C)$ are the Hankel matrices of the Catalan numbers and

$$m_{ij} = \begin{cases} F_3 = 2 & \text{if } i = j = 1 \quad \text{or} \quad i = j = k; \\ F_4 = 3 & \text{if } i = j \in \{2, \dots, k-1\}; \\ F_2 = 1 & \text{if } i = j + 1 \quad \text{or} \quad i = j - 1; \\ F_0 = 0 & \text{otherwise.} \end{cases}$$

Proof. This follows by the same method as in the proofs of Propositions 32 and 34, considering the ladder graph L_{2k-2} . The following is the triangular snake graph associated to L_{2k-2} .



An easy computation shows that the path matrix of the previous triangular snake graph is the desired one. \square

4.2 Some identities in not straight snake graphs

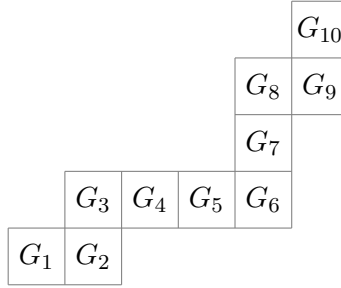
Building on our previous results regarding Fibonacci numbers and ladder graphs, this chapter extends our analysis to more general snake graphs. We introduce a new notation to define a snake graph in terms of the length of each maximal straight subgraph within this graph, allowing us to study their properties and relationships with Fibonacci numbers.

Definition 38. Given a snake graph \mathcal{G} , a *chain* \mathcal{G}_{ij} is a subgraph of \mathcal{G} that forms a maximal ladder graph. That is, there are no other ladder graphs within \mathcal{G} that contain \mathcal{G}_{ij} , and \mathcal{G}_{ij} consists of the tiles G_k , where $i \leq k \leq j$. The *length* $l(\mathcal{G}_{ij})$ of a chain \mathcal{G}_{ij} is defined as the number of tiles it contains, *i.e.*, $l(\mathcal{G}_{ij}) = j - i + 1$.

Based on Definition 38, we can describe a snake graph using its horizontal and vertical chains. We denoted by $\mathcal{G}_h(l_1, l_2, \dots, l_k)$ the snake graph in which l_i represents the length of the horizontal chains when i is odd, and the length of the vertical chains when i is even. Conversely, $\mathcal{G}_v(l_1, l_2, \dots, l_k)$ denotes the snake graph where l_i represents the length of the vertical chains if i is odd, and the length of the horizontal chains if i is even. The concept of a chain can be analogously defined for triangular snake graphs.

Remark 39. The only snake graph that contains a chain of length 1 is the one formed by a single tile, denoted as $\mathcal{G} = G_1 = \mathcal{G}_h(1) = \mathcal{G}_v(1)$. In all other cases, the chains have a length of at least 2. However, in some computations (see Lemma 41), initial chains of length 0 or 1 may appear. By convention, we define $\mathcal{G}_h(0, l_2, \dots, l_k) = \mathcal{G}_v(l_2 - 1, l_3, \dots, l_k)$ and $\mathcal{G}_h(1, l_2, \dots, l_k) = \mathcal{G}_v(l_2, l_3, \dots, l_k)$. Similarly, we set $\mathcal{G}_v(0, l_2, \dots, l_k) = \mathcal{G}_h(l_2 - 1, l_3, \dots, l_k)$ and $\mathcal{G}_v(1, l_2, \dots, l_k) = \mathcal{G}_h(l_2, l_3, \dots, l_k)$.

Example 40. The snake graph $\mathcal{G}_h(2, 2, 4, 3, 2, 2)$ is illustrated below:



This snake graph consists of 3 horizontal chains:

$$\begin{aligned}\mathcal{G}_{1,2} &= \{G_1, G_2\}, \\ \mathcal{G}_{3,6} &= \{G_3, G_4, G_5, G_6\}, \\ \mathcal{G}_{8,9} &= \{G_8, G_9\},\end{aligned}$$

and 3 vertical chains:

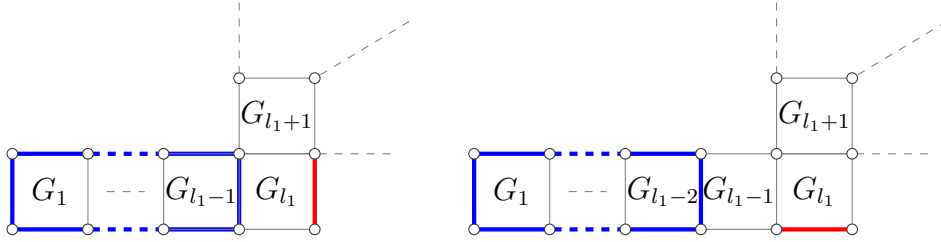
$$\begin{aligned}\mathcal{G}_{2,3} &= \{G_2, G_3\}, \\ \mathcal{G}_{6,8} &= \{G_6, G_7, G_8\}, \\ \mathcal{G}_{9,10} &= \{G_9, G_{10}\}.\end{aligned}$$

This chain description allows for recursive combinatorial counting using Fibonacci numbers, as illustrated in the following lemma.

Lemma 41. *Let \mathcal{G} be a snake graph represented by $\mathcal{G}_h(l_1, l_2, \dots, l_k)$, where $l_i \geq 2$ for all $i \in \{1, \dots, k\}$. The number of perfect matchings $m(\mathcal{G})$ of \mathcal{G} is given by the recurrence relation:*

$$m(\mathcal{G}) = F_{l_1} m(\mathcal{G}_v(l_2 - 1, l_3, \dots, l_k)) + F_{l_1+1} m(\mathcal{G}_v(l_2 - 2, l_3, \dots, l_k)).$$

Proof. We classify all perfect matchings of the snake graph $\mathcal{G} = \mathcal{G}_h(l_1, l_2, \dots, l_k)$ by considering the edge incident to the lower right vertex of the tile G_{l_1} . This edge can either be a vertical or an horizontal edge, as illustrated in the following figure:



If a perfect matching contains the vertical edge, then the edges on the left part of the snake graph are chosen in $m(L_{l_1-1}) = F_{l_1+1}$ ways, and the edges of the remaining part of the snake graph are chosen in $m(\mathcal{G}_v(l_2 - 2, l_3, \dots, l_k))$ ways. Analogously, for a perfect matching that contains the horizontal edge, the edges on the left part of the snake graph are chosen in $m(L_{l_1-2}) = F_{l_1}$ ways, and the edges of the remaining part of the snake graph are chosen in $m(\mathcal{G}_v(l_2 - 1, l_3, \dots, l_k))$ ways. Therefore, the total number of perfect matchings $m(\mathcal{G})$ is given by the recurrence:

$$m(\mathcal{G}) = F_{l_1} m(\mathcal{G}_v(l_2 - 1, l_3, \dots, l_k)) + F_{l_1+1} m(\mathcal{G}_v(l_2 - 2, l_3, \dots, l_k)),$$

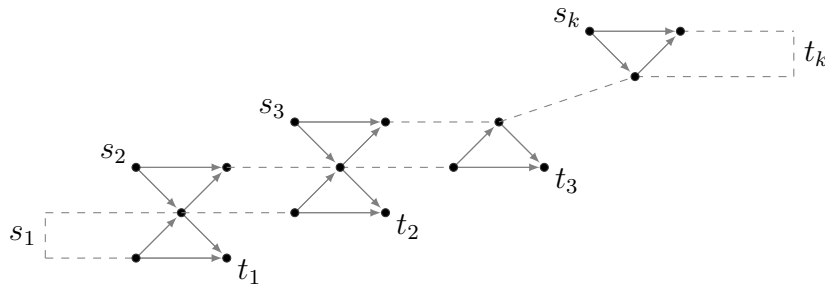
as desired. \square

Remark 42. As a preliminary observation, we note that a recurrence for $m(\mathcal{G}_v(l_1, \dots, l_k))$ can be derived in a manner analogous to the one presented in Lemma 41. This is because $\mathcal{G}_v(l_1, l_2, \dots, l_k)$ is a reflection of $\mathcal{G}_h(l_1, l_2, \dots, l_k)$, implying that both graphs are structurally identical, just mirrored. Consequently, we have

$$m(\mathcal{G}_v(l_1, l_2, \dots, l_k)) = m(\mathcal{G}_h(l_1, l_2, \dots, l_k)).$$

Additionally, for any snake graph, the number of perfect matchings can be expressed as a sum of products of Fibonacci numbers. In § 4.1, we observed that the entries of the path matrix for the triangular snake graph associated with a ladder graph are Fibonacci numbers. This leads us to inquire whether it is possible to express the entries of the path matrices for general snake graphs in terms of Fibonacci-like expressions.

Proposition 43. *Let $M_{st} = (m_{ij})_{1 \leq i, j \leq k}$ be the path matrix associated to the following triangular snake graph:*



derived from the snake graph $\mathcal{G}_h(l_1, 2, l_2, 2, \dots, 2, l_k)$ such that edge contraction of the $k-1$ vertical chains results in the hourglass graphs \mathbb{X}_i , $i \in \{1, \dots, k-1\}$. Then, the elements of M_{st} are given by:

$$m_{ij} = \begin{cases} F_{l_{i+1}}F_{l_{j+1}} \prod_{r=i+1}^{j-1} F_{l_r} & \text{if } i < j; \\ F_{l_{i+2}} & \text{if } i = j; \\ F_2 & \text{if } i = j + 1; \\ F_0 & \text{otherwise.} \end{cases}$$

Proof. Since the vertical chains of the snake graph $\mathcal{G}_h(l_1, 2, l_2, 2, \dots, 2, l_k)$ are all of length two, and their edge contraction results in an hourglass graph, the number of paths from vertex s_i to vertex t_i , for $i \in \{1, \dots, k\}$, is equal to the Fibonacci number $F_{l_{i+2}}$, as the graph corresponds to a triangular snake graph associated to a ladder graph L_{l_i} . On the other hand, there is only $F_2 = 1$ path from vertex s_i to vertex t_j if $i - j = 1$, and $F_0 = 0$ if $i - j > 1$.

Finally, to address the remaining case, we note that a path from s_i to s_j for $i < j$ must pass through the necks of the intermediate hourglass graphs $\mathbb{X}_i, \dots, \mathbb{X}_{j-1}$, so does not pass through the arrows incident to the source or sink vertices of these graphs. Specifically, there are $F_{l_{i+1}}$ paths from s_i to the neck n_i of \mathbb{X}_i , $F_{l_{j+1}}$ paths from n_{j-1} to t_j , and F_{l_r} paths from n_{r-1} to n_r for each $r \in \{i+1, \dots, j-1\}$. Therefore, the total number of paths

is $m_{ij} = F_{l_{i+1}}F_{l_{j+1}} \prod_{r=i+1}^{j-1} F_{l_r}$, as desired. \square

Remark 44. In Proposition 43, the associated triangular snake graph can be obtained by applying either the contraction defined in Definition 22 or the opposite contraction considered in Remark 29. For general snake graphs where not all edge contractions of vertical chains result in hourglass graphs, it is still possible to express path matrices in terms of Fibonacci numbers. However, these cases involve applying both the original and opposite contractions simultaneously. Consequently, some entries in the path matrices may be determinants of smaller path matrices, which themselves can be described using Fibonacci numbers.

In § 4.1, we examined path matrices whose entries were expressed in terms of Fibonacci or Catalan numbers, with determinants also yielding Fibonacci numbers. We now explore an example where the determinant corresponds to a different well-known numerical sequence.

Proposition 45. *Let P_n be the n -th Pell number defined recursively by $P_n = 2P_{n-1} + P_{n-2}$ for $P_0 = 0$, $P_1 = 1$ and $n \geq 2$. Let $M_k = (m_{ij})$ and $M'_k = (m'_{ij})$ be the $k \times k$ matrices*

defined as follows:

$$m_{ij} = \begin{cases} F_5 & \text{if } i = j = 1; \\ F_5 + F_3 & \text{if } i = j \in \{2, \dots, k\}; \\ F_4 F_3 & \text{if } i = 1 \text{ and } j > 1; \\ (F_4 + F_2) F_3 & \text{if } i \neq 1 \text{ and } i < j; \\ F_2 & \text{if } i = j + 1; \\ F_0 & \text{otherwise.} \end{cases}$$

and

$$m'_{ij} = \begin{cases} F_5 & \text{if } i = j = 1; \\ F_5 + F_3 & \text{if } i = j \in \{2, \dots, k-1\}; \\ F_4 F_3 & \text{if } i = 1 \text{ and } 1 < j < k; \\ (F_4 + F_2) F_3 & \text{if } i \neq 1, j \neq k \text{ and } i < j; \\ F_4 + F_2 & \text{if } 1 < i < k \text{ and } j = k; \\ F_4 & \text{if } i \in \{1, k\} \text{ and } j = k; \\ F_2 & \text{if } i = j + 1; \\ F_0 & \text{otherwise.} \end{cases}$$

Then,

$$\det M_k = P_{2k+1} \quad \text{and} \quad \det M'_k = P_{2k}.$$

Proof. Consider the snake graph \mathcal{G} associated to the continued fraction $[2, 2, \dots, 2, 2]$.

This snake graph consists of $2k-1$ chains, each of length 3; that is, $\mathcal{G} = \mathcal{G}_h(\underbrace{3, 3, \dots, 3, 3}_{(2k-1)\text{-times}})$.

From a direct inspection of Figure 9, we can observe that the matrix M_k corresponds to the path matrix associated to the triangular snake graph $\mathcal{T}_{\mathcal{G}}$. Furthermore, by directly

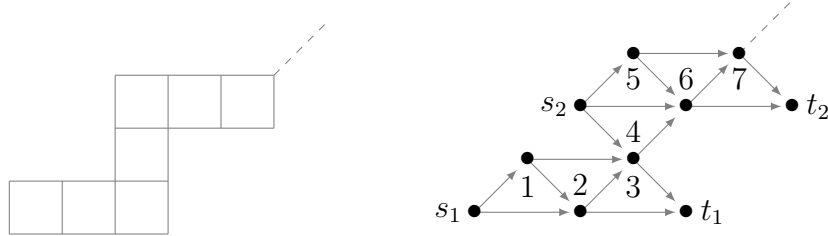
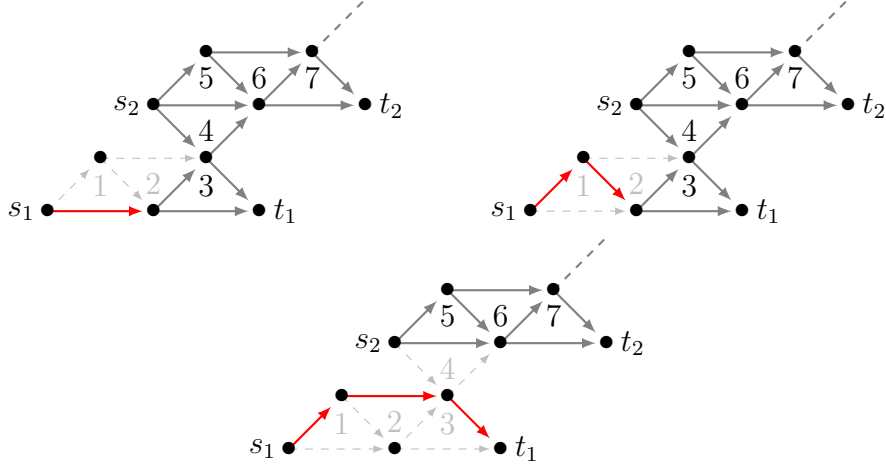


Figure 9: Pell Snake graph and its corresponding triangular snake graph.

examining the routes in $\mathcal{T}_{\mathcal{G}}$, we observe that the paths from s_1 to t_1 fall into one of the following three cases:



The first two cases (from left to right) correspond to the number of routes in the triangular snake graph associated to $\mathcal{G}_v[3, 3, \dots, 3, 3]$, while the remaining case corresponds to the number of routes in the triangular snake graph associated to $\mathcal{G}_h[3, 3, \dots, 3, 3]$. Therefore, the number of routes in $\mathcal{T}_{\mathcal{G}}$ (or perfect matchings in \mathcal{G}) satisfies the same recurrence relation as the Pell numbers. Similarly, if we consider the continued fraction $[2, 2, \dots, 2, 2]$, the associated path matrix is M'_k , whose determinant corresponds to the previously mentioned Pell number. Thus, the desired result is proved. \square

Example 46. Consider the snake graphs \mathcal{G}' and \mathcal{G} associated to the continued fractions $[2, 2, 2, 2, 2]$ and $[2, 2, 2, 2, 2, 2]$, respectively. The number of perfect matchings of \mathcal{G}' and \mathcal{G} are given by

$$m(\mathcal{G}') = \det M'_3 = \begin{vmatrix} F_5 & F_4 F_3 & F_4 \\ F_2 & F_5 + F_3 & F_4 + F_2 \\ F_0 & F_2 & F_4 \end{vmatrix} = P_6 = 70,$$

and

$$m(\mathcal{G}) = \det M_3 = \begin{vmatrix} F_5 & F_4 F_3 & F_4 F_3 \\ F_2 & F_5 + F_3 & (F_4 + F_2) F_3 \\ F_0 & F_2 & F_5 + F_3 \end{vmatrix} = P_7 = 169.$$

5 Future work

This work has showed that, for all snake graphs, the number of perfect matchings can be expressed as a sum of products of Fibonacci numbers. Additionally, we have explored how certain well-known sequences, such as the Fibonacci and Pell sequences, can be characterized through determinants of matrices with Fibonacci number entries. A natural question arises: can other sequences be described similarly? For instance, the Fibonacci

and Pell numbers are particular cases within the broader Markov sequence. It would be interesting to study whether there are families of matrices that can effectively describe this sequence in an analogous manner.

Furthermore, previous works such as [25] and [26] established a relationship between the continued fraction associated with a snake graph, the number of perfect matchings, and the framework of cluster algebras. Specifically, if \mathcal{G} is the snake graph of a cluster variable within a cluster algebra arising from a surface, then each cluster variable \mathbf{x} is represented by a formula involving the perfect matchings of \mathcal{G} . Through the bijections introduced in this paper, we can reinterpret these expressions as products of arrow labels within paths of the k -route associated with a perfect matching, combined with labels of contraction edge vertices that are not part of any path in the route. This suggests a potential avenue for further exploration, where such combinatorial interpretations may offer new insights into the algebraic structures underlying cluster variables and related sequences.

Acknowledgements

I would like to express my sincere gratitude to Alfredo Nájera Chávez for his invaluable comments, suggestions, and corrections on earlier drafts of this work. Additionally, I thank Timothy Magee for his insightful observations, particularly regarding the use of Hankel notation in Proposition 32. Their contributions have significantly improved the quality of this paper.

References

- [1] F. Ardila. Algebraic and Geometric Methods in Enumerative Combinatorics. *Handbook of enumerative combinatorics*, Boca Raton, CRC Press, 2015.
- [2] F. Ardila, and R. Stanley, Tilings*. *The Mathematical Intelligencer*, 32: 32–43, 2010. [doi:10.1007/s00283-010-9160-9](https://doi.org/10.1007/s00283-010-9160-9).
- [3] A. Benjamin, N. Cameron, and J. Quinn. Fibonacci determinants - A combinatorial approach. *The Fibonacci Quarterly*, 45, 2005.
- [4] L. M. Bregman. Some properties of nonnegative matrices and their permanents. *Soviet Math. Dokl.*, 211: 27–30, 1973.
- [5] S. Butler, J. Ekstrand, and S. Osborne. Counting Tilings by Taking Walks in a Graph. *Springer International Publishing*, 153–176, 2020.
- [6] M. Ciucu. Perfect matchings of cellular graphs. *J. Algebraic Combinatorics*, 5: 87–103, 1996.
- [7] N. Elkies, G. Kuperberg, M. Larsen, and J. Propp. Alternating sign matrices and domino tilings. *Journal of Algebraic Combinatorics*, 1:111–132, 1992.
- [8] S.-P. Eu and T.-S. Fu. A Simple Proof of the Aztec Diamond Theorem. *Electronic Journal of Combinatorics*, 12:8, 2005.

- [9] M. Fisher and H. Temperley. Dimer problem in statistical mechanics – an exact result. *Philosophical Magazine*, 68:1061–1063, 1992.
- [10] N. Garnier and O. Ramaré. Fibonacci numbers and trigonometric identities. *The Fibonacci Quarterly*, 1–7, 2008.
- [11] I. Gessel and X. Viennot. Determinants, Paths, and Plane Partitions. *Preprint*, 1989.
- [12] P. W. Kasteleyn. The statistics of dimers on a lattice I. The number of dimer arrangements on a quadratic lattice. *Physica*, 27: 1209–1225, 1992.
- [13] M. Katz and C. Stenson. Tiling a $(2 \times n)$ -Board with Squares and Dominoes. *Journal of Integer Sequences*, 12, 2009.
- [14] D. Klarner and J. Pollack. Domino tilings of rectangles with fixed width, *Discrete Mathematics*, 32 (1): 45–52, 1980
- [15] T. Koshy. Fibonacci and Lucas Numbers with Applications. *Pure and applied mathematics: a Wiley-Interscience series of texts, monographs, and tract*, New York, 2001.
- [16] J. Layman. The Hankel Transform and Some of its Properties. *Journal of Integer Sequences*, 4: 11, 2001.
- [17] B. Lindström. On the vector representations of induced matroids. *Bulletin of the London Mathematical Society*, 5: 85–90, 1973.
- [18] L. Lovász and M. Plummer. Matching Theory. *North-Holland Mathematics Studies*, Rutgers University, New Brunswick, NJ, U.S.A, 1986.
- [19] C. Melo. Emparejamientos perfectos, álgebras de conglomerado y algunas de sus aplicaciones (Master’s thesis). *Universidad Nacional de Colombia*, Bogotá, Colombia, 2019.
- [20] G. Musiker, R. Schiffler, and L. Williams. Positivity for cluster algebras from surfaces. *Advances in Mathematics*, 227: 2241–2308, 2011.
- [21] G. Musiker, R. Schiffler, and L. Williams. Bases for cluster algebras from surfaces. *Compositio Mathematica*, 149: 217–263, 2013.
- [22] N. Sloane. The On-Line Encyclopedia of Integer Sequences. *published electronically*, 1964.
- [23] R. Stanley. Enumerative Combinatorics, Volume 2. *Cambridge Studies in Advanced Mathematics*, vol. 62, Cambridge University Press, 1999.
- [24] R. Stanley. Catalan Numbers. *Cambridge University Press*, Cambridge, 2015.
- [25] I. Çanakçı and R. Schiffler. Snake graph calculus and cluster algebras from surfaces. *Journal of Algebra*, 382: 240–281, 2013.
- [26] I. Çanakçı and R. Schiffler. Cluster algebras and continued fractions. *Compositio Mathematica*, 154(3): 565–593, 2018.